



Universitetet
i Stavanger

DET TEKNISK-NATURVITENSKAPELIGE FAKULTET

MASTEROPPGAVE

| | |
|--|--|
| Studieprogram/spesialisering: Master i informasjonsteknologi, automatisering og signalbehandling | Vårsemesteret, 2017 Åpen / Konfidensiell |
| Forfatter: Alexander Kvale Moene | (signatur forfatter) |
| Fagansvarlig: Mahdieh Khanmohammadi,, Kjersti Engan Veileder(e): | |
| Tittel på masteroppgaven: Extracting coronary arteries in angiographic images Engelsk tittel: Extracting coronary arteries in angiographic images | |
| Studiepoeng: 30 | |
| Emneord: | Sidetall: 43 + vedlegg/annet: Matlabcode .zip Stavanger, 15.06.2017 dato/år |

Extracting coronary arteries in angiographic videos

Alexander Kvale Moene

15 June 2017

Summary

This master thesis has as propose to extract coronary arteries form angiographic video. With several stability issues with the easy to implement established functions in the time domain and other methods that is far too extensive to implement in the short time span. The focus turned to create a method that is easy to use over an image sequence by using information gathered in the time domain.

Uneven illumination is dealt with by homomorphic filtering and static noise as bone and cables are removed by subtraction the median image found in the time domain. The image is then over segmented by using SLIC superpixels that cluster around the arteries.

By tracking the movement in the images over time it is possible to divide the image into a dynamic part and static part. Then by observing noise in the static part the noise in the dynamic part can be kept at acceptable levels and the threshold level can be automatically adjusted each frame if needed by observing noise in the static area. From this function three binary images are made with different noise levels.

The 1st image is combined with the superpixel image and the occupancy in each superpixel determine if the superpixel area is of interest or not. After the initial segmentation is done a growing superpixel segment is seeded a from the edges of the static dynamic mask as the contrast agent needle is always connected to the edge of the screen and expands by observing the neighbouring superpixels.

The binary images are then combined with the fully grown superpixel image and through an incremental growth based on the binary images the final segmentation is achieved.

The result is a method that simplified the problem to a contrast problem and can be improved with Watershed method and active contours to increase the segmented area.

Table of Contents

| | | |
|-------|--|----|
| 1 | Introduction | 5 |
| 2 | Experimentation | 6 |
| 2.1 | Top hat filtering | 6 |
| 2.2 | Frangi hessian filtering | 7 |
| 2.3 | Otsu's method..... | 9 |
| 2.4 | Other methods | 10 |
| 2.4.1 | Directional filter bank | 10 |
| 2.4.2 | Histogram equalization | 10 |
| 2.4.3 | Transitional image processing | 10 |
| 3 | Proposed method..... | 11 |
| 3.1 | Pre-processing..... | 11 |
| 3.1.1 | Homomorphic filtering | 12 |
| 3.1.2 | Median subtraction | 13 |
| 3.1.3 | Static Dynamic mask | 14 |
| 3.1.4 | Adaptive global thresholding based on Static Dynamic mask..... | 15 |
| 3.2 | Segmentation and post processing | 18 |
| 3.2.1 | Super pixel processing..... | 19 |
| 3.2.2 | Three stage growing process based on binary images | 21 |
| 3.3 | Improvement by Water shedding | 23 |
| 3.4 | Improvement by Active contours, Chan vese | 24 |
| 5 | Results..... | 25 |
| 5.1 | Patient 1: Session 5 | 25 |
| 5.2 | Patient 2: Session 4 | 27 |
| 5.3 | Patient 4: Session 2 | 29 |
| 5.4 | Patient 5: Session 2 | 31 |
| 5.5 | Patient 6: Session 5 | 33 |
| 5.6 | Patient 7: Session 7 | 35 |
| 5.7 | Patient 9: Session 4 | 37 |
| 5.8 | Patient 1: Session 5, Active contour adjustment | 39 |
| 5.9 | Patient 1: Session 5, Watershed adjustment..... | 40 |
| 6 | Conclusion | 41 |
| 7 | References | 42 |

1 Introduction

Cardiovascular disease in Norway was the most common form of death with 11,613 deaths this amounts to 28,54% of total death in 2015 [1]. In later years, the severity of heart disease has steadily declined to be quarter compared to 1970s and half of the level in 2000. However, the last 5 years (2011-2016) the decline have been around 10%. The large decline in the past is attributed to reduction of smoking in Norway and low recent decline is attributed to the unhealthy lifestyle with little exercise and increasing weight. [2]

Coronary arteries disease (iskemisk hjertesykdom, norwegian) is the most frequent cause of death in cardiovascular diseases 36,29%, or 4,214 deaths and 10,36% of all causes of deaths in 2015. [3]

This study is in regards to the detecting coronary arteries, these are the vessels providing blood to the heart muscle and tissue. Visualisation of the coronary arteries are done with in X-ray angiography video and the injection of a contrast agent. The contrast agent provides a darkening of the vessel and several images are taken in sequence it is possible to see how the contrast agent unfolds in the arteries over time.

The primary problem has been defined in the assignment text as:

Accurate visualization of blood vessels, has a major role in assessing failures however vessel detection has been a challenge due to low contrast between the vessels and the background in the angiogram, unknown and deformable shape of the coronary arteries tree, crossing and overlapping of the vessels, and overlapping shadows of other present organs in human cavity such as bones and lungs.

This master project is a part of an ongoing project on estimating the blood flow velocity by only using image and video processing techniques on x-ray angiograms. The study is a collaboration between invasive cardiology ward of Stavanger University Hospital (SUS) and the department of electrical engineering and computer science at the University of Stavanger. The data includes angiography videos of 40 patients which are captured at SUS. [4]

The goal is to present a simple and effective, robust automatic method for detecting the coronary arteries in angiography images

2 Experimentation

Some of the method that was found in publication [5]. The study in gives an overview of the methods used. However as creating artificial intelligence and many model approaches are unavailable or too complex. Instead some of the simpler accessible methods was tested to see how they worked in the time domain.

2.1 Top hat filtering

An alternative method for equalizing uneven illumination is by top hat filtering with morphological operator [6]

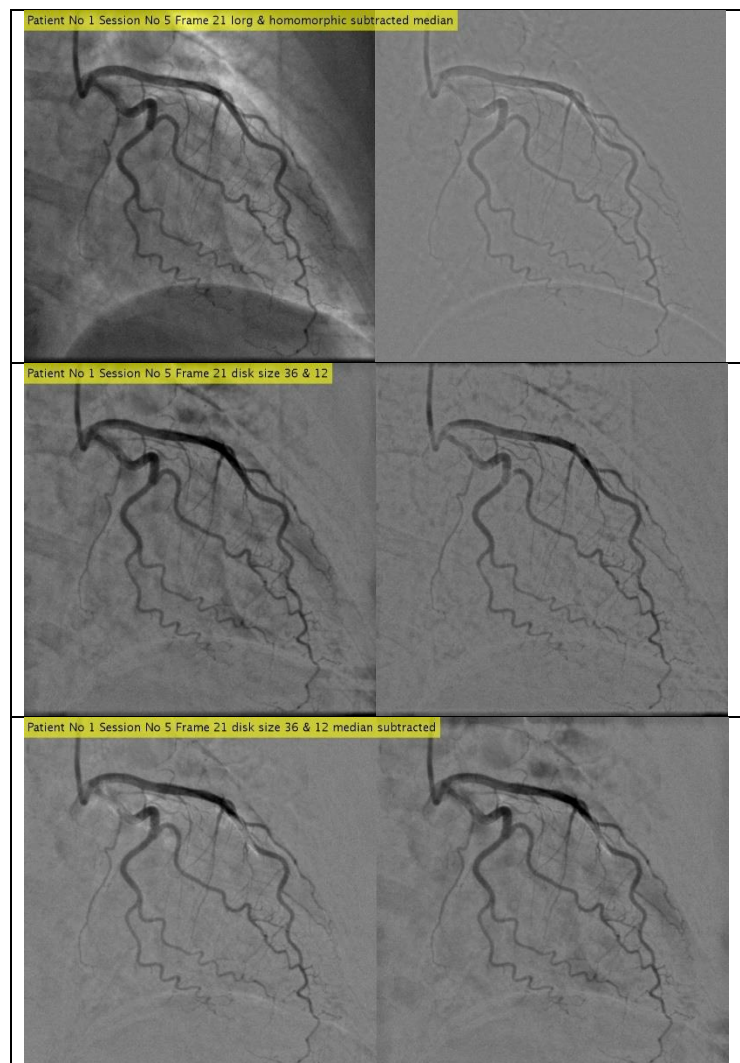
$$I_{Tophat} = I_{org} - Imopen(I_{org}, se)$$

In this case a disk operator with size 36 and 12 was used.

The results of the top hat filtering were that in general produced little noise and the noise that was produce was in the shape of large blobs.

When subtraction the median image this caused noise to be removed in images with a large morphological operator and introduce noise in image with a small operator.

This method was discarded due to the nature of the noise having a blob shape. proposed method it is not a worse method than homomorphic imaging and may serve better as an image for active contours due to the nature of the noise.



2.2 Frangi hessian filtering

This is a method that is looking for tubular elements by multiscale vessel enhancement methods.

The method comprises of the following steps: [7]

Convolution filtering of a 2nd order partial derivate, hessian filter

Perform eigenvalue decomposition

Order eigenvalues and compute the vessel classification

Repeat using different scales and combine the results

The convolutional filter is made by creating a kernel of a second derivate Gaussian. This is one of the weaknesses as the second derivate is the size of the mask grows quickly

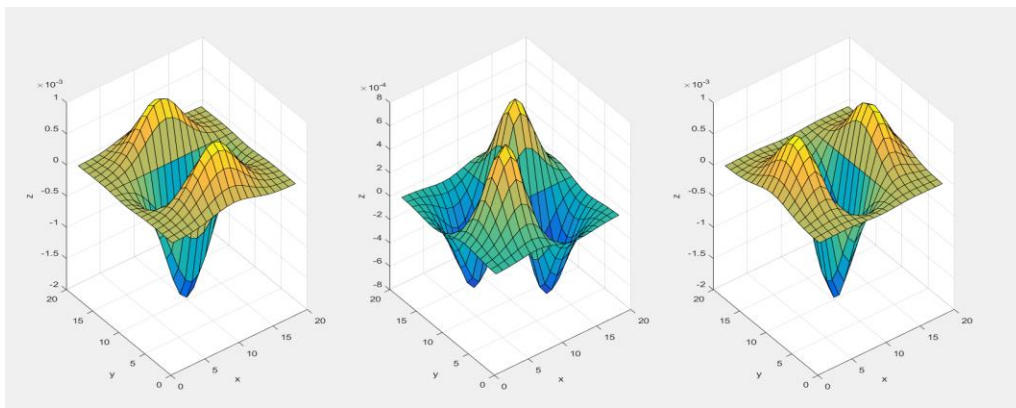


Figure 2.2-1 D Gaussxx, D Gaussxy, D Gaussyy filter kernels to obtain hessian Dxx, Dxy Dyy Sigma = 3.

$$D_{xx}(x, y) = \sum_{i=1}^N \sum_{j=1}^M I(i, j) * D_{Gaussxx}(x - i, y - j)$$

$$D_{xy}(x, y) = \sum_{i=1}^N \sum_{j=1}^M I(i, j) * D_{Gaussxy}(x - i, y - j)$$

$$D_{yy}(x, y) = \sum_{i=1}^N \sum_{j=1}^M I(i, j) * D_{Gaussyy}(x - i, y - j)$$

$$E_{igenvalues}(\lambda_1, \lambda_2) = f(D_{xx}, D_{xy}, D_{yy})$$

$$Rb = \left(\frac{\lambda_2}{\lambda_1} \right)^2, \text{ Rb indicates a tubular shape}$$

$$S2 = \lambda_1^2 + \lambda_2^2, \text{ S2 indicates a round shape}$$

$$I_{Frangi} = e^{\frac{-Rb}{2\beta_1^2}} - e^{\frac{-S2}{2\beta_2^2}}$$

lower β_1 will increase the emhpises on tubular shapes

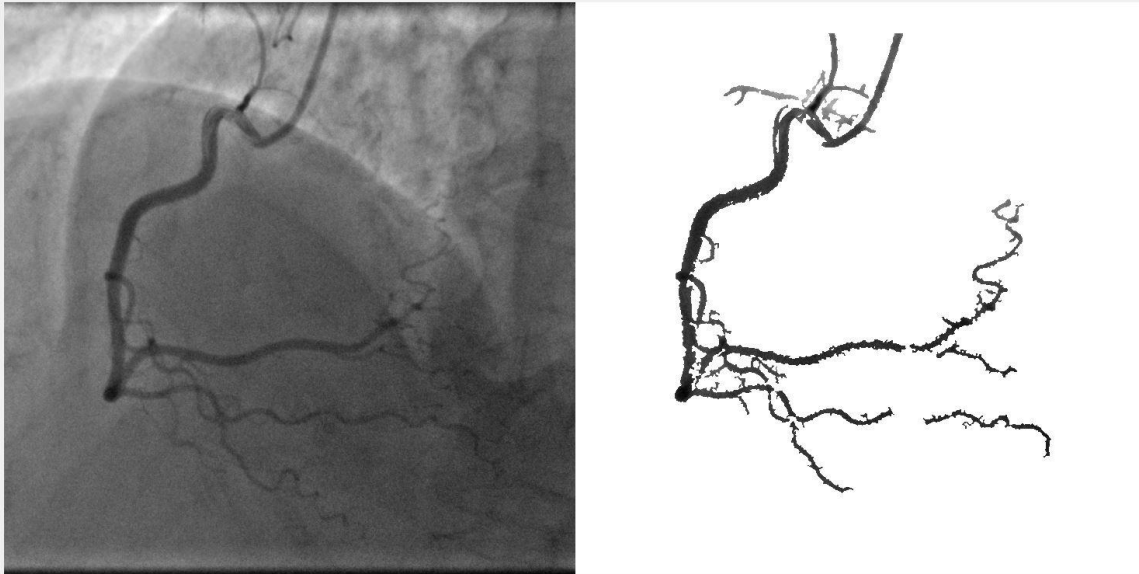
lower β_2 will increase the emhpises on round shapes

Precise Frangi hessian extraction demands a lot of micromanagement both within a dataset and between to get a proper extraction due the variation of vascular patterns. As the purpose of this assignment was to make a robust method is was therefore abandoned.

As Beta 1 and Beta 2 are bias values they were difficult to find good values unless brute forced and inspected manually.

The implementation of this function was not created in this assignment with the original implementation available in the math works forum. [8]

Frequent problems with treshodling image results in disjointed segments



Sgementation grows out of proportins or include unwanted information

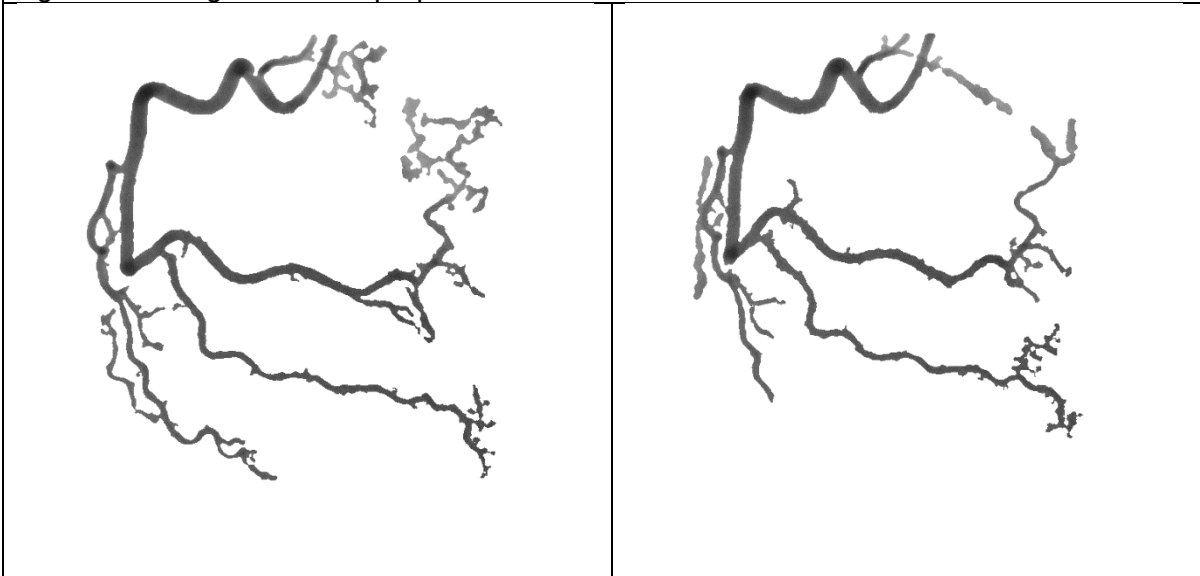


Figure 2.2-2 Frangi hessian flaws, broken segment and noise

2.3 Otsu's method

Defined as: [9]

$$\sigma_w = \omega_0(t)\sigma_0^2(t) + \omega_1(t)\sigma_1^2(t)$$

Class probability:

$$\omega_0(t) = \sum_{i=0}^{t-1} p(i) \quad \omega_1(t) = \sum_{i=t}^L p(i) \quad , \quad \omega_0(t) + \omega_1(t) = 1$$

$$\sigma_b^2 = \sigma^2 - \sigma_w^2 = \omega_0(\mu_0 - \mu_T)^2 + \omega_1(\mu_1 - \mu_T)^2 = \omega_0(t)\omega_1(t)[\mu_0(t) - \mu_1(t)]^2$$

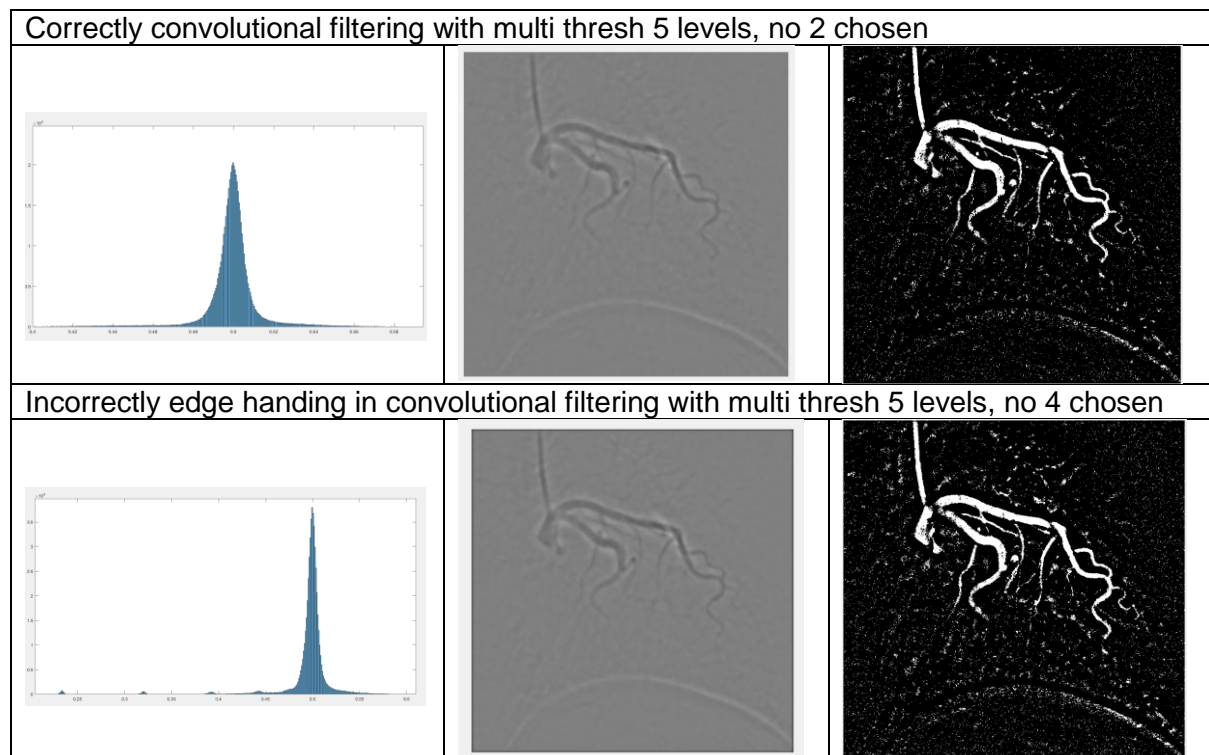
Class expectations:

$$\mu_0(t) = \sum_{i=0}^{t-1} i \frac{p(i)}{\omega_0} \quad \mu_1(t) = \sum_{i=t}^{L-1} i \frac{p(i)}{\omega_1} \quad \mu_T = \sum_{i=0}^{L-1} ip(i)$$

The thresholding algorithm calculates probability for each intensity level then iterates over all threshold values until the greatest threshold by updating μ_i og ω_i and updating σ_b^2 , the largest value of is the threshold value.

As Otsu's method is used in [10] it should be mentioned that this method is not appropriate for homomorphic images as after homomorphic filtering the image takes the form of a Gaussian distribution and simple processing does not change shape of the histogram in a notable way that would give local minimum and Otsu's method will return the mean of the image. If several threshold values are to be found they are more related to a % of the shape rather than a useful thresholding value.

While it is possible to get decent binarizations with this method it is very time consuming as it is required to low pass filter the image one or more times with different kernels and check several number of levels in the multi thresh function and then each of those. This may be necessary to verify frame by frame. If you do not remember to pad your image when you perform convolutional filtering the artefacts will introduce local minimums that may make the method to appear to be working however this must be avoided.



2.4 Other methods

Some other methods were tested.

2.4.1 Directional filter bank

Initially there was a desire to implement the work found in [10] however as Gabor filtering [11] was easy to implement and works in a similar way but with emphases on edges. While it was possible to detect smaller veins with Gabor filtering, when thresholding the Gabor image this tend to leave large artefacts around the arteries as a suitable threshold value was difficult to automate.

2.4.2 Histogram equalization

Histogram equalization was used as a comparison in [10] however it dose suffer from the same flaws that Otsu's method is in that is have problems in the early frames and stretching a Gaussian function serves little purpose, it doses however perform well in a fully saturated image.

2.4.3 Transitional image processing

Based on an observation in the time domain that the image sequence could be reconstructed using the transitional images the following could be estimated.

$$I_{org} \approx I_{summed}(i) = \Delta I_{org}(i) + I_{summed}(i - 1)$$

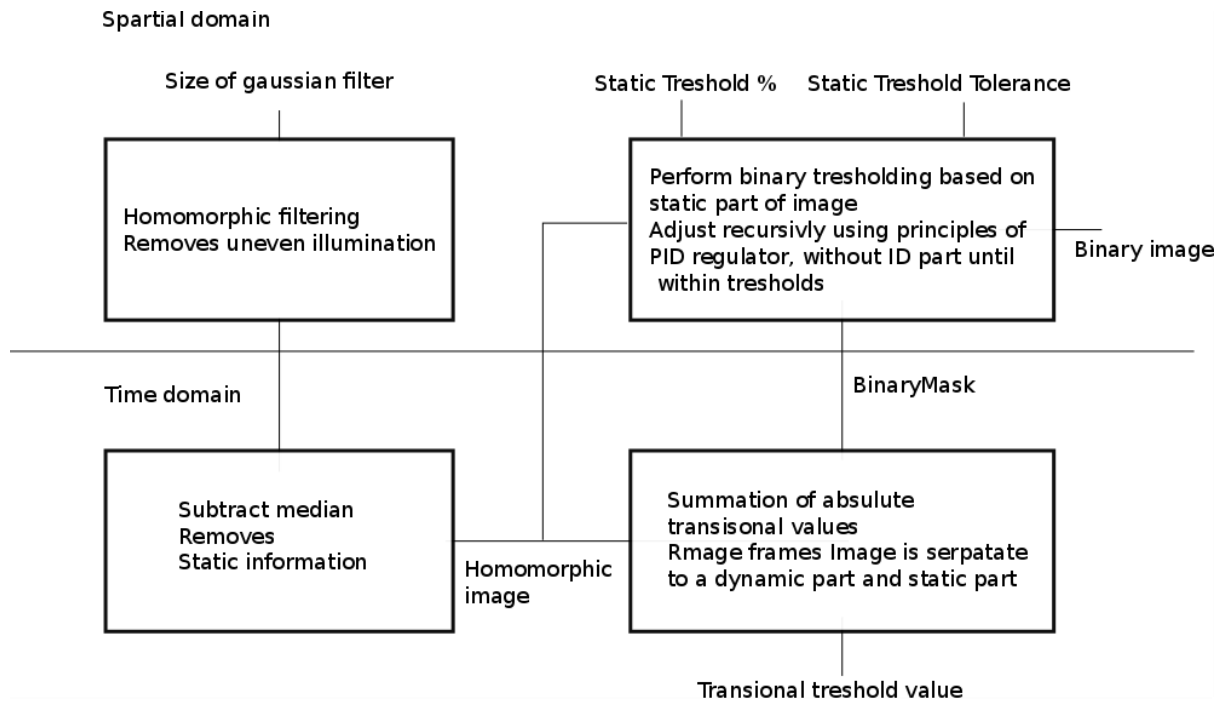
$$\Delta I_{org}(i) = I_{org}(i) - I_{org}(i - 1)$$

Simple convolutional filtering was done to $\Delta I_{org}(i)$ to a lesser amount of success. It may however be explored further if the need of variables is required for pattern recognition or neural networks.

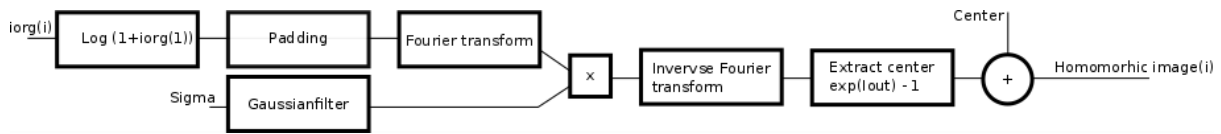
3 Proposed method

The proposed method introduces an adaptive threshold method and growing segment method using super pixels based on observation in the time domain. The method is inspired by the need of a more suitable threshold function than Otsu's method as this performs too unreliable and a desire for more control than achieved in Frangi hessian.

3.1 Pre-processing



3.1.1 Homomorphic filtering



$$I_{Log} = \ln(1 + I_{org})$$

Fourier transform:

$$I_{FFT} = F\{Log\}$$

$$F(k, l) = \sum_{n=1}^N \sum_{m=1}^M f(n, m) e^{-j2\pi(\frac{kn}{N} \frac{lj}{N})}$$

$$I_{FFTfiltered} = I_{FFT} * H$$

Inverse Fourier transform:

$$I_{out} = F\{I_{FFTfiltered}\}^{-1}$$

$$f(n, m) = \frac{1}{NM} \sum_{k=1}^N \sum_{l=1}^M F(k, l) e^{j2\pi(\frac{kn}{N} \frac{lj}{N})}$$

$$I_{homo} = ((e^{-I_{out}}) - 1) + center$$

Homomorphic filtering is used to remove uneven illumination in an image by filtering away the low frequency component in the logarithmic image. To avoid artefacts a Gaussian shaped filter is used as well as the image is padded. As the DC component is removed the image is centered around a new mean.

The implementation of this function was not created in this assignment with the original implementation available in the mat works form. [12] [13]

| Original image: iorg, size(MxN) | Padded image size(2M+2N+1) |
|-------------------------------------|-------------------------------|
| | |
| Homomorphic image: ihomo, size(MxN) | FFT filter Gaussian, Sigma 25 |
| | |

Figure 3.1-1 Stages of homomorphic filtering

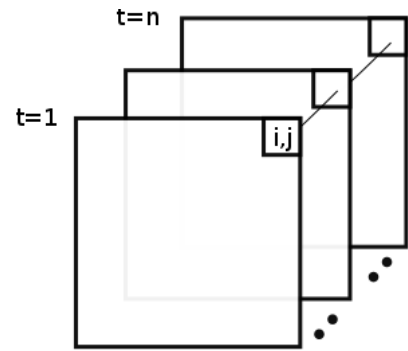
3.1.2 Median subtraction

$$\text{MedianImage}(i, j) = \text{median}(\text{ihomo}(i, j), t), \quad t = 1 \text{ to } n$$

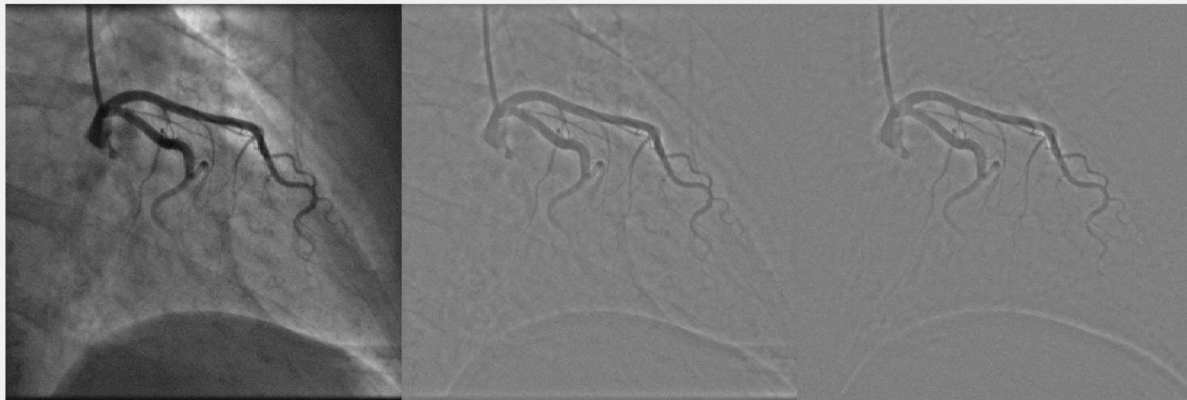
$$\text{Isubbackground}(a) = \text{Ihomo}(a) - \text{MedianImage} + \text{center}$$

The median image is created by finding the median value for each pixel location trough time.

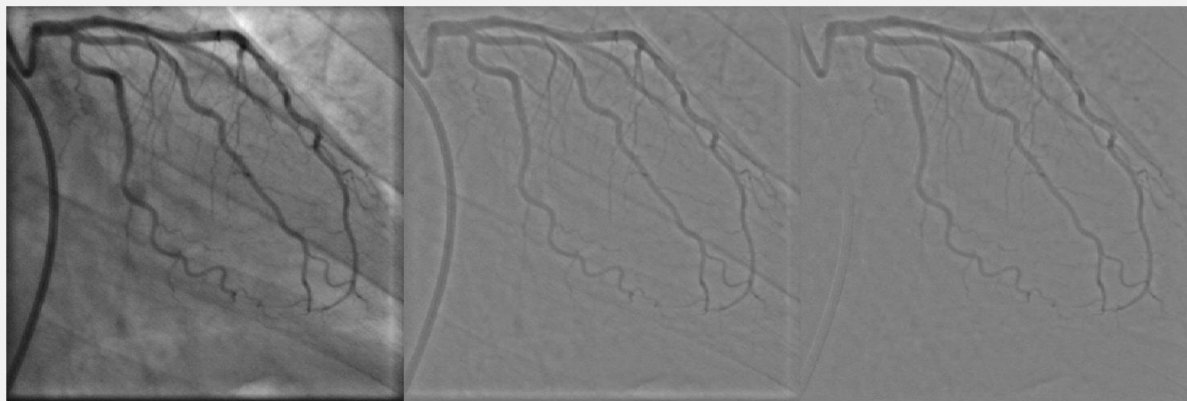
Median subtraction is used to remove the background components as spines and ribs. The method dose this very well and introduces little noise. However, for this method to work the camera must remain stationary for best results



Large ribs are removed



Cables from contrast equipment



Spines are removed

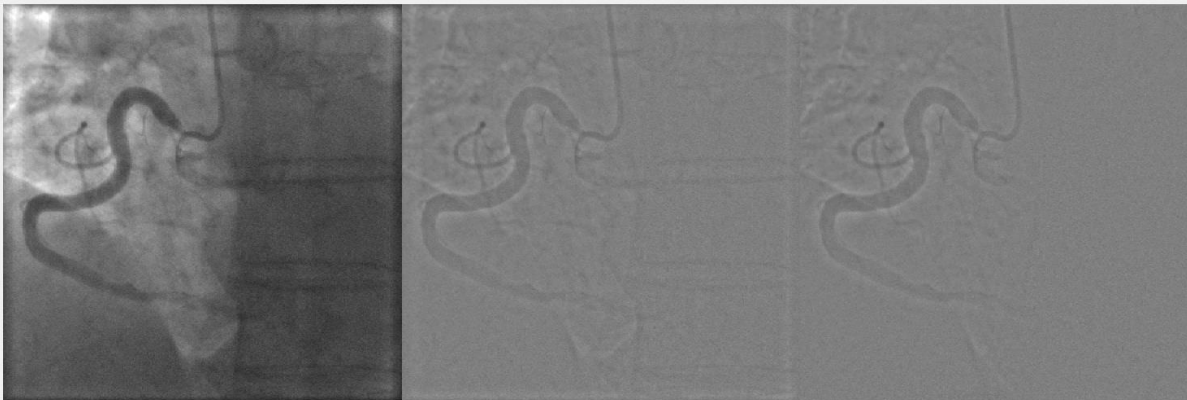


Figure 3.1-2 Static noise is easily removed from image by subtracting the median image

3.1.3 Static Dynamic mask

$$I_{Conv}(n, m, t) = \sum_{i=1}^N \sum_{j=1}^M I(i, j, t) * h(n - i, m - j), h = 11 \times 11 \text{ gaussian } \sigma = 2$$

$$I_{trans}(t) = I_{Conv}(t) - I_{Conv}(t - 1)$$

$$SDM_{ini} = SDM_{ini} | \sum_{d=1}^{T-1} abs(I_{trans}(t)) > threshold$$

$$SDM_{dilate} = imdilate(SDM_{ini}, morphoperator)$$

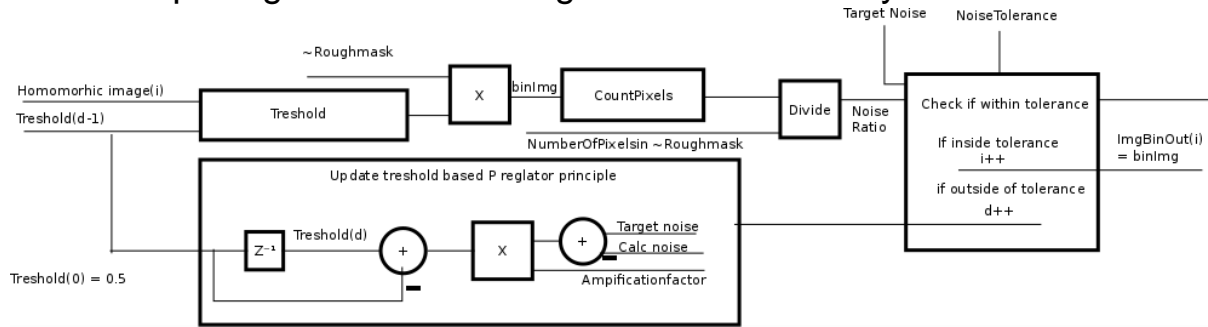
$$StaticDynamicMask = extractlargestobject(SDM_{dilate})$$

The method of creating the static dynamic mask uses the basic image processing methods convolutional filtering with a Gaussian kernel, arbitrary global threshold and a binary morphological dilation operation with a disk operator. The initial purpose was to find seed points for the segmentation algorithms however observations indicated that the area was very suitable to find a global threshold value.



Figure 3.1-3 Black = Static part, White = Dynamic part

3.1.4 Adaptive global thresholding based on Static Dynamic mask



$$binImg = f(threshold(d), image(i)) * (1 - StaticDynamiMask)$$

$$Masksize = \sum_{m=1}^M \sum_{n=1}^N (1 - StaticDynamiMask(m, n))$$

$$NoiseRatio = \frac{\sum_{m=1}^M \sum_{n=1}^N BinImg(m, n)}{Masksize}$$

$$Threshold(d) = Threshold(d - 1) + ((targetNoise - NoseRatio) * Amplificationfactor)$$

This method was implemented as a robust binarization method was needed and commonly used method binarizing images is not suitable or intended for homomorphic images.

By observing image values in the dynamic and static mask in an early frame with no information the image values appear to be Gaussian distributed with same sigma in both dynamic and static area. Then observing further into the time lapse when the contrast fluid is injected the resulting image 3 distinct Gaussian functions can be observed

- Noise, centred around 0.5, sharp sigma
- Vessels, centred below 0.5 with wide sigma.
- Vessel artefacts, centred above 0.5 with wide

Since the values in dynamic and static mask the assumption that static noise ≈ 0 due to median subtraction and however dynamic noise as breathing and heartbeats causing ribs and dark areas to not removed by median subtraction.

Since the vessels appear in the lowest values this allows the proposed method to find a global threshold values by observe the static area and threshold based on the amount of noise that is observed to update the threshold value the difference from desiered noise and calculated noise is used a variable. This is not unlike a PID regulator without a ID. This is done to avoid having to store values during brute forcing the correct threshold value. The result is a well performing binarization that generates homogenous binarization images over the entire image sequence.

Histogram values of dynamic static values

Blue = static, orange = dynamic

Final segmentation of 5% image,
Values inside the static dynamic mask
Blue = segmented area, orange = other

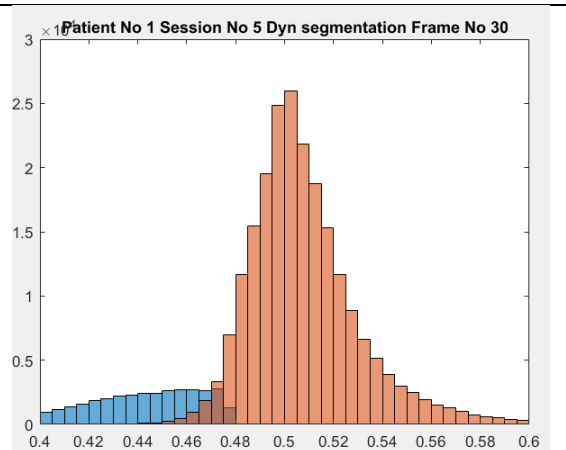
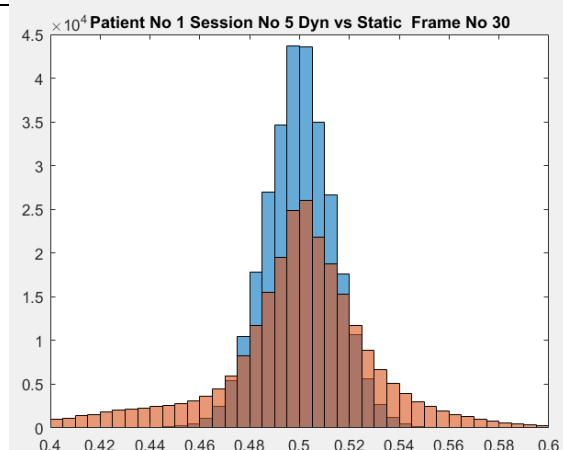
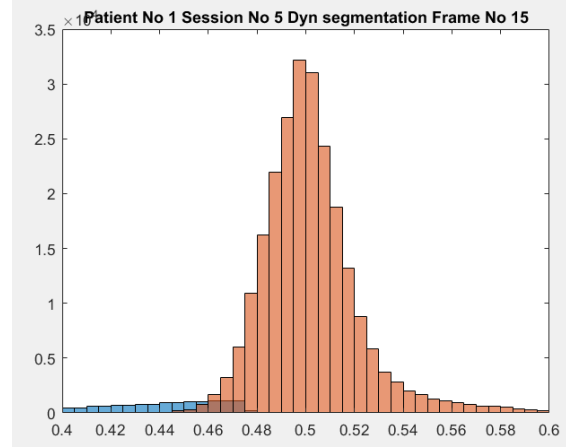
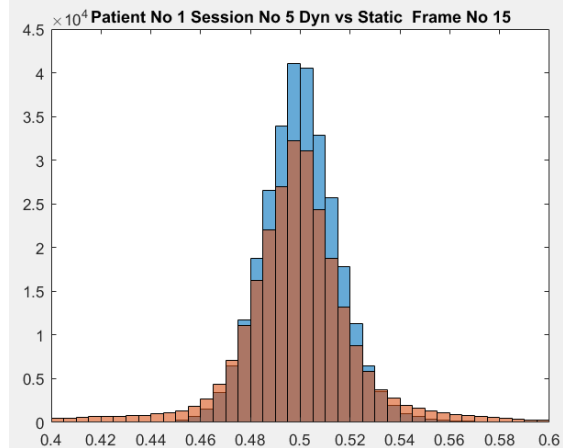
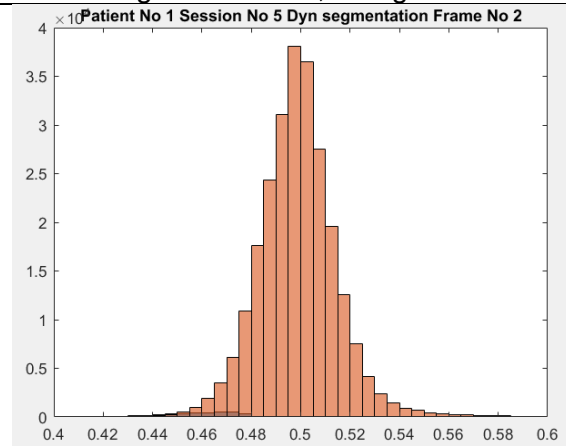
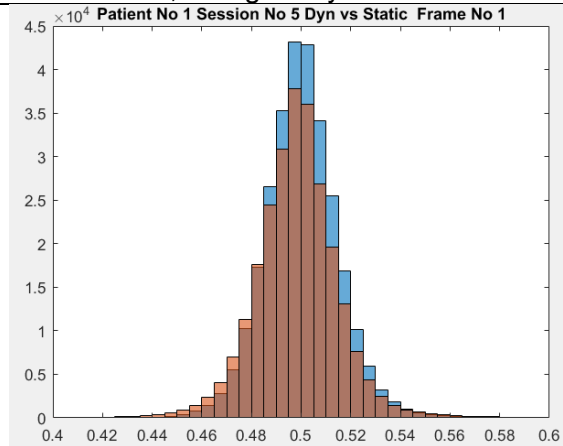


Figure 3.1-4 Histogram comparison

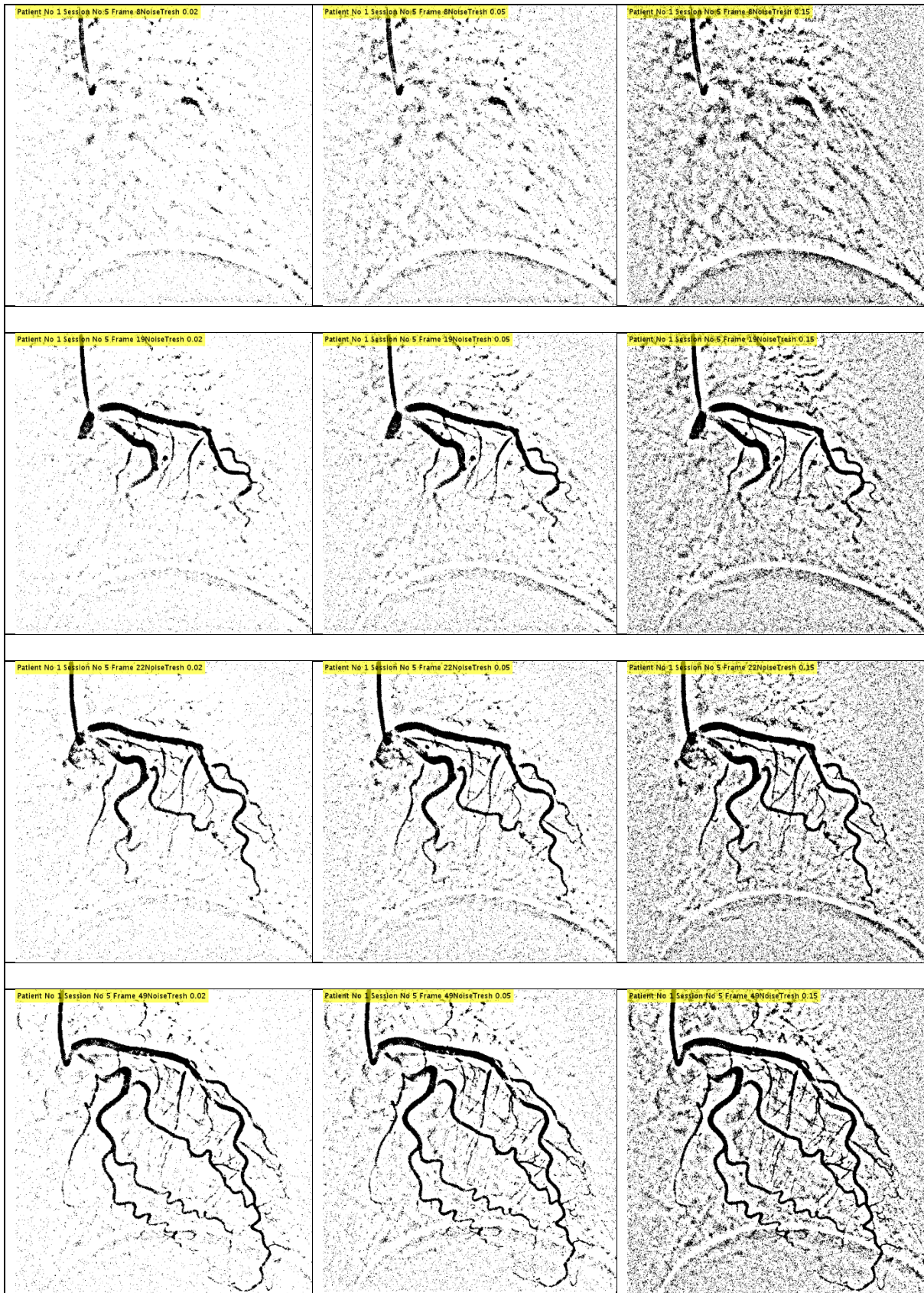
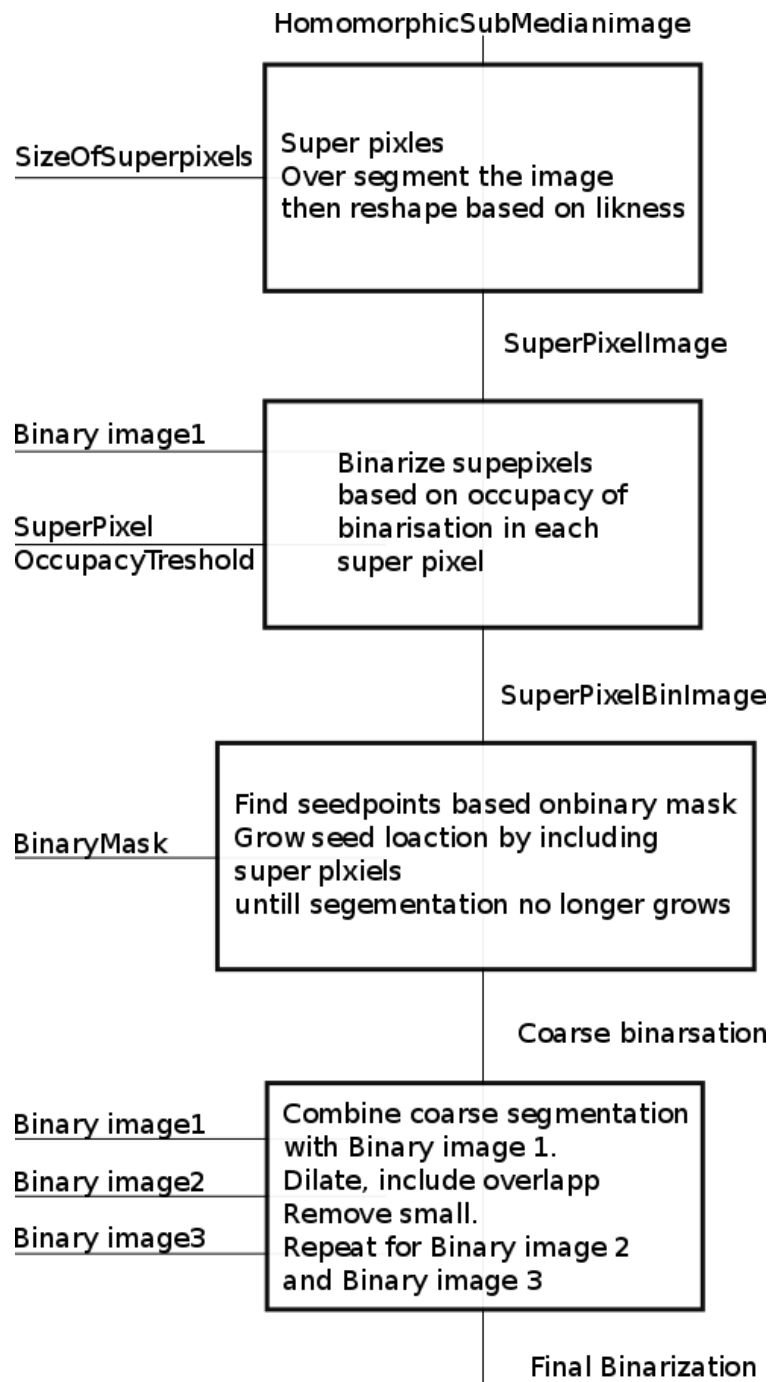


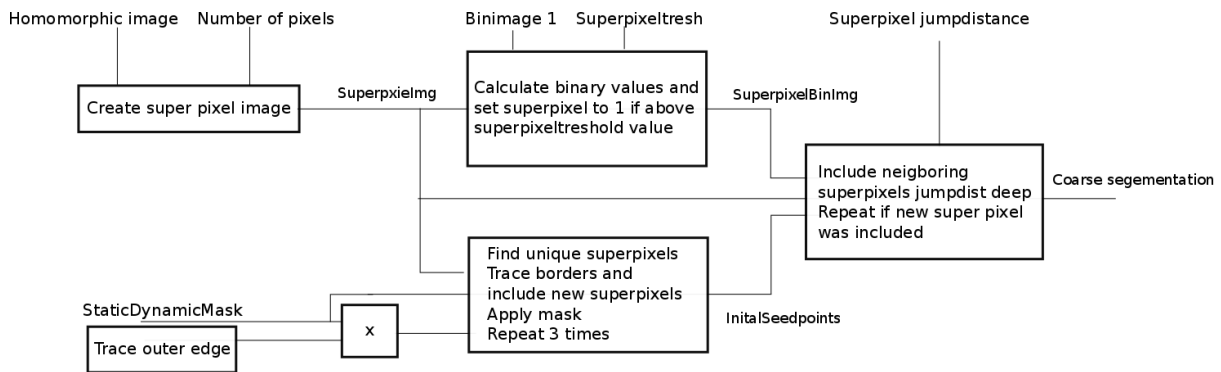
Figure 3.1-5 The proposed method generates equal binarization quality over the entire image sequences.

3.2 Segmentation and post processing

The initial segmentation is done by processing superpixels



3.2.1 Super pixel processing



The seed location is set to grow from the edges of the image based observation as the needle that supplies the contrast agent is always connected to the edge of the image. Should the camera be off centred in a way that cuts of the vessel and leaves a large gap between the two parts this can be detected.

The super pixel method is an over segmentation method that divides the image into several areas then processes them based on the similarity of the pixels in the cluster. The superpixel method is based on the SLIC method [14] using 20 iterations with the number of segments to be M+N, the non-fixed size was found suitable as the size of the images ranges from 736x736 to 1000x1000.

$$Size_i = \sum_1^m \sum_1^n Superpixel(m, n) == i$$

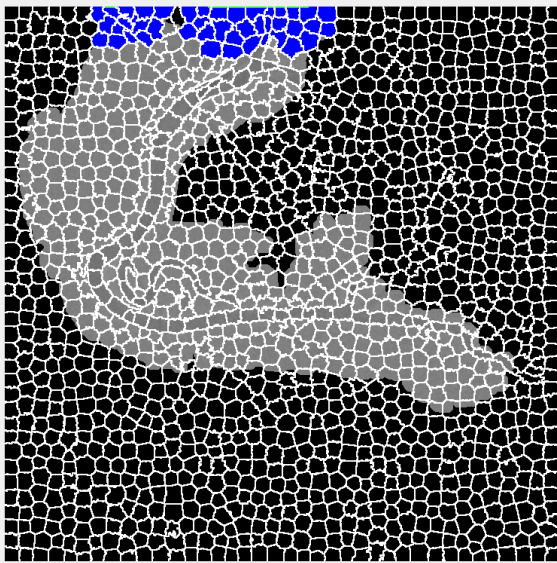
$$Occupacy_i = \sum_1^m \sum_1^n Superpixel(m, n) * binimage1(m, n) == i$$

$$SuperpixelBin_i = 1, \text{ for } \frac{Occupacy_i}{Size_i} > superpixeltresh \text{ else } 0$$

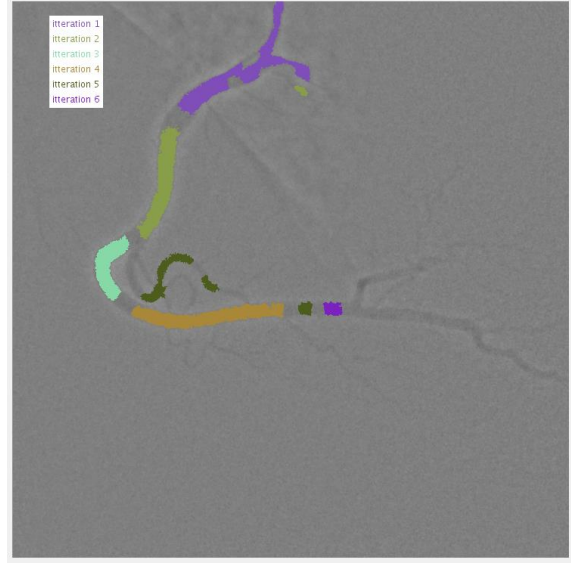
The 1st binary image is selected by its properties to be able to exclude noise and provides good initial seed point. Super pixel threshold value and jump distance is adjusted as needed.

The growing of the superpixel are done by tracing the segmented image then applying the mask to the super pixel and finding unique super pixels then extracting those and repeating until no super pixels are added.

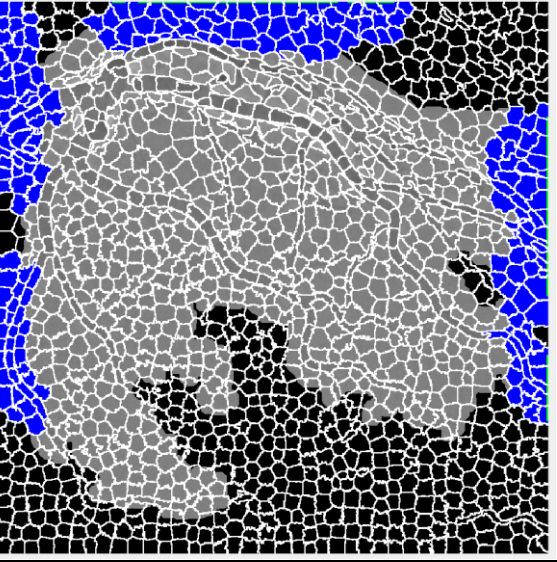
Initial Seed area



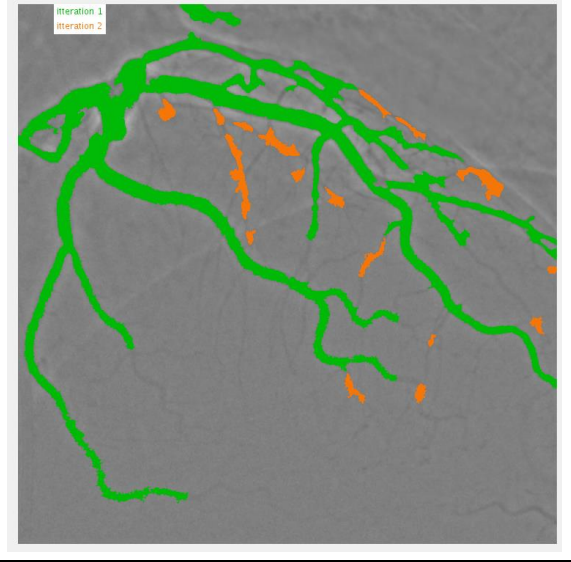
After growing from seedpoint



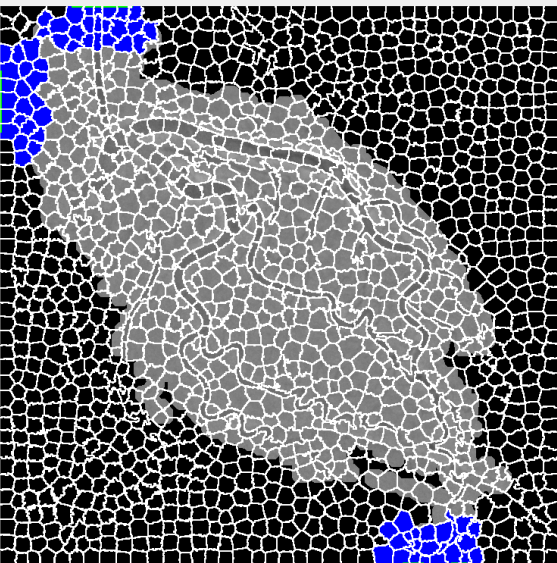
Initial Seed area



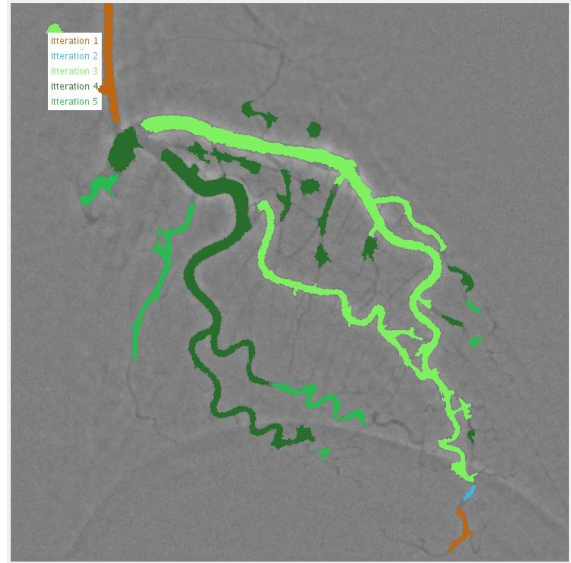
Multiple seed points adds some noise



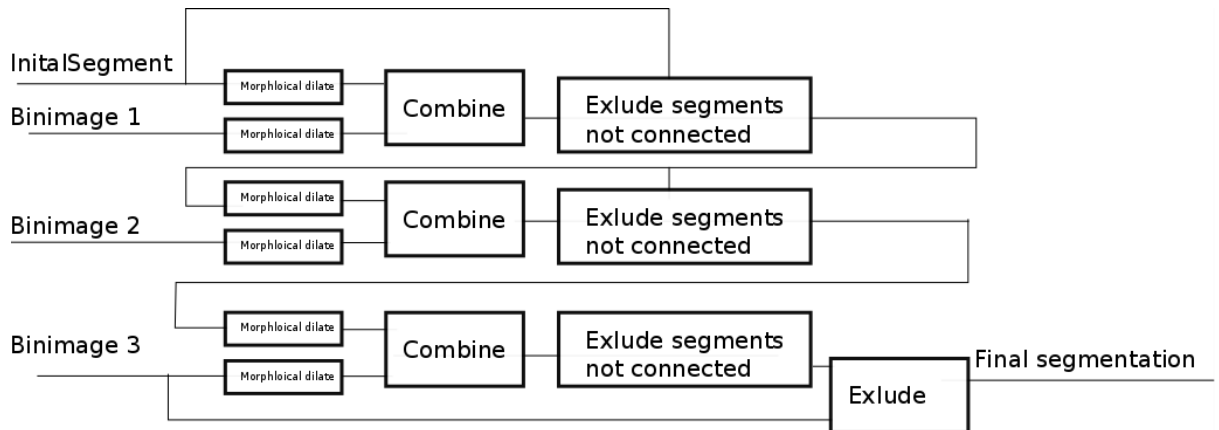
Initial Seed area



Multiple seed points correct the initial mask



3.2.2 Three stage growing process based on binary images



$$Seg_1 = (dilate(Seg_{ini}) \cup dilate(BinImg_1)) \cap Seg_{ini}$$

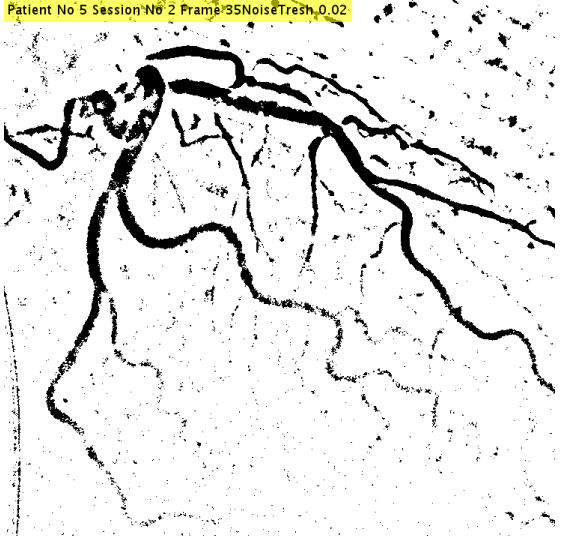

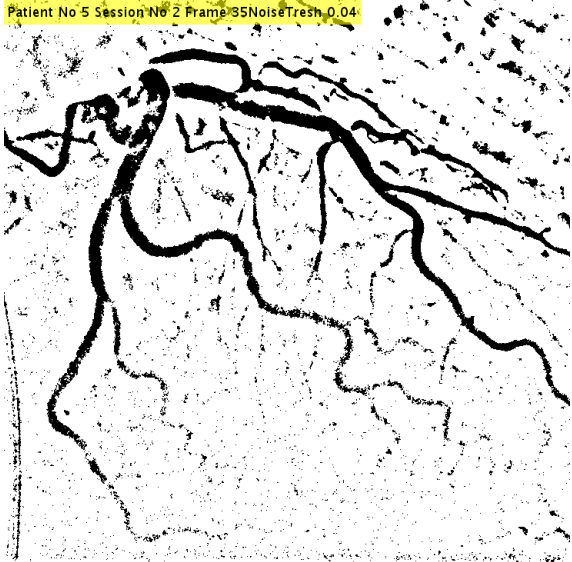

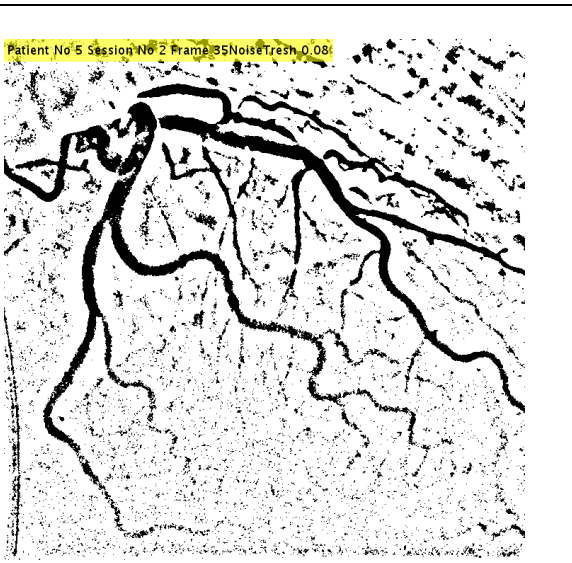

$$Seg_i = (dilate(Seg_{i-1}) \cup dilate(BinImg_i)) \cap Seg_{i-1}$$

$$Finalsegmenttion = Seg_i \cap BinImg_i$$

The initial image found from super pixels are morphological dilated with a morphological dilated binary image. Then small objects are filtered away and the area the overlaps with the initial area in anyway are kept. The same procedure is conducted two more time as after observation more than 3 resulted in excess noise in many cases.

The 3rd binary image is found by exploring different values of noise. When the 1st and 3rd image is found the typical 2nd binary image s in the middle of this.

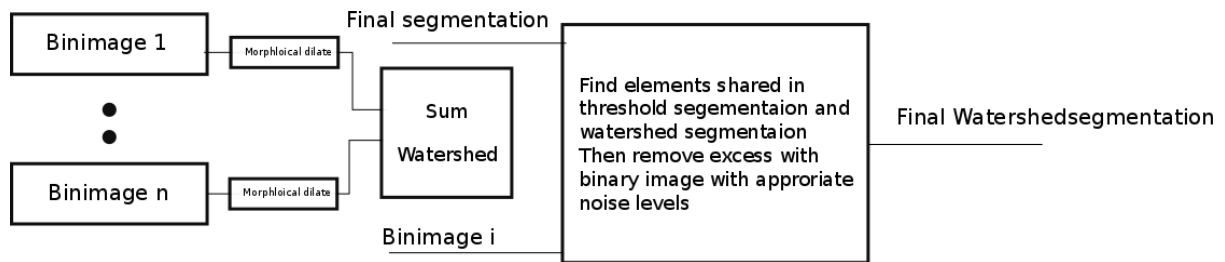
This method is inspired by the same way as frangi hessian and coronary tree extraction method [15] in the way it combines different iterations to slowly grow the segmentation rather than all at once.

| | |
|---|--|
| <p>Bin 1</p> <p>Patient No 5 Session No 2 Frame 35 NoiseTresh_0.02</p>  | <p>Coarse segmentaion</p> <p>Patient No 5 Session No 2 Frame 35 SuperpixelSegmentation</p>  |
| <p>Bin 2</p> <p>Patient No 5 Session No 2 Frame 35 NoiseTresh_0.04</p>  | <p>Mid segmentaion</p> <p>Patient No 5 Session No 2 Frame 35 MidSegmentation</p>  |
| <p>Bin 3</p> <p>Patient No 5 Session No 2 Frame 35 NoiseTresh_0.08</p>  | <p>Final segmentaion</p> <p>Patient No 5 Session No 2 Frame 35 FinalSegmentation</p>  |

3.3 Improvement by Water shedding

The watershed method finds watershed ridge lines based on the gradient in an image by treating light pixels as high elevations and dark pixel low elevations. Different labels are created as the threshold is incremented and labels are either separated or combined depending on the gradient [16]

While not fully explored, and implemented this method resulted in improvement in some images at the expense of introducing some noise and the method has the potential to improve the final segmentation



The image for watershed is constructed by summation of several processed binary images with different noise levels then watershed. The watershed segmenting elements that overlaps into the final segmentations are chosen. The chosen elements are multiplied with a binary image that contains the desired vessels vs noise.

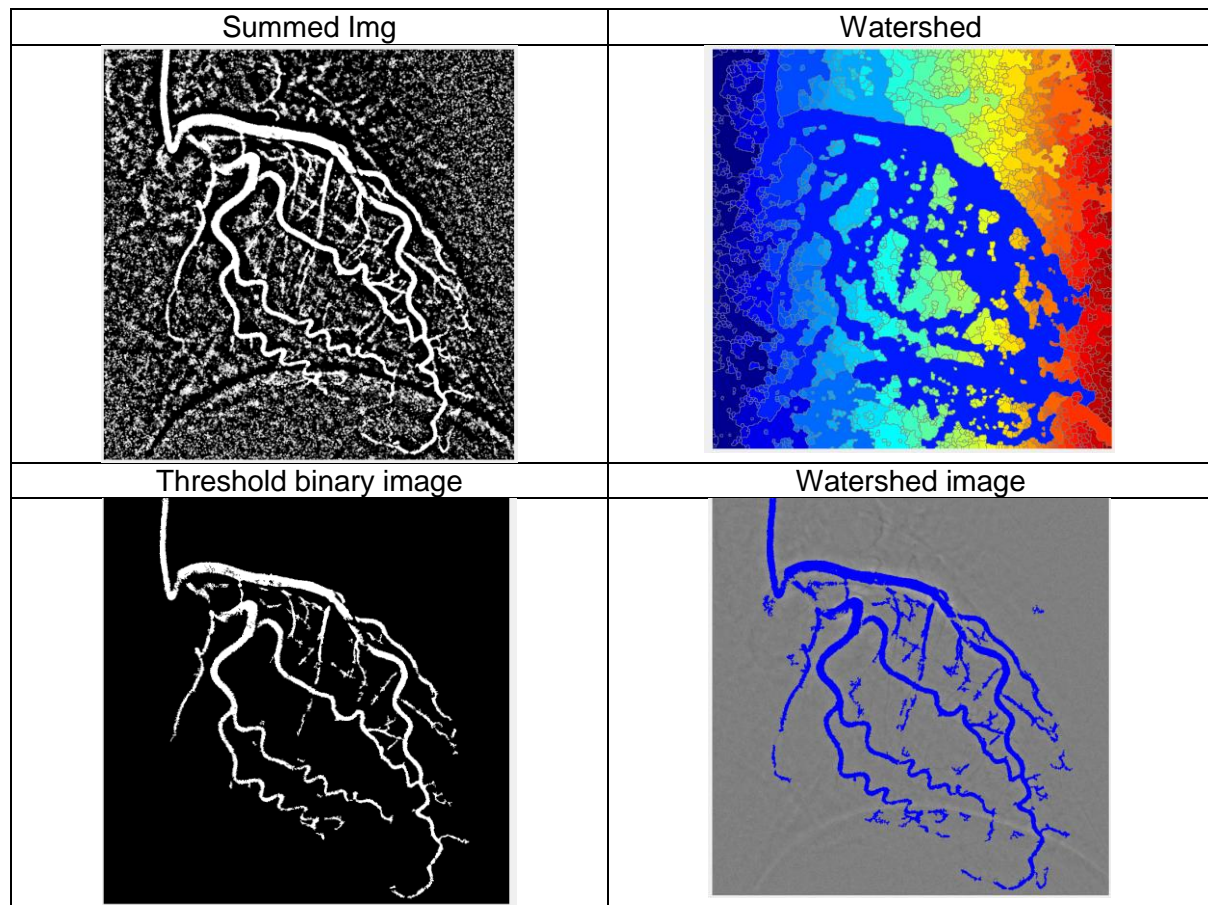


Figure 3.3-1 The summed image is created by the summation of 1 to 21 % noise with 2% increments. The large body is found Bywater shedding and the watershed image is produced by the 11% noise image.

3.4 Improvement by Active contours, Chan vese

Active contour is a growing segments method that grows or contracts based on the surrounding pixels around and initial mask. This is done by using a contraction bias Chan vese [17]

The use of active contours on the homomorphic image , with the final segmentaion image as a seed mask only had an enhancement effect on the results and demanded some adjustment in the contraction bias to work properly. The effect is rather random as well and the only way to find an appropriate bias value is by testing different values.

4 Results

Vessel and background annotation done by Mahdiah Khanmohammadi,

4.1 Patient 1: Session 5

Comment: Image had very clear contrast and allowed low noise trash to

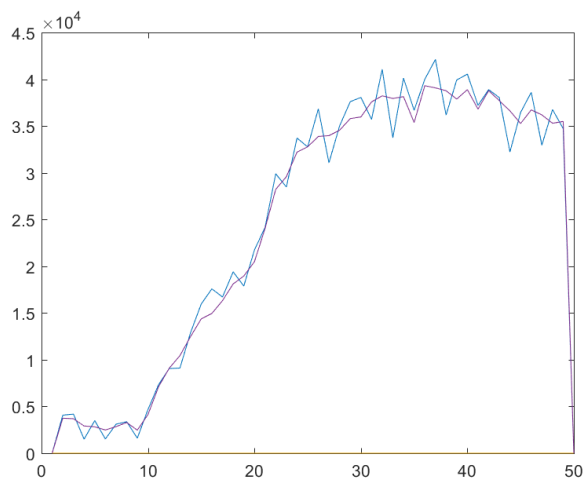
Parameters:

| | |
|------------------------------|------|
| Homomorphic Sigma | 25 |
| BinImgNoiseTresh1 | 0.01 |
| BinImgNoiseTresh2 | 0.02 |
| BinImgNoiseTresh3 | 0.05 |
| SupersixelOccupancyThreshold | 0.25 |
| Number of smoothing | 0 |
| Dynmasktresh | 5.5 |

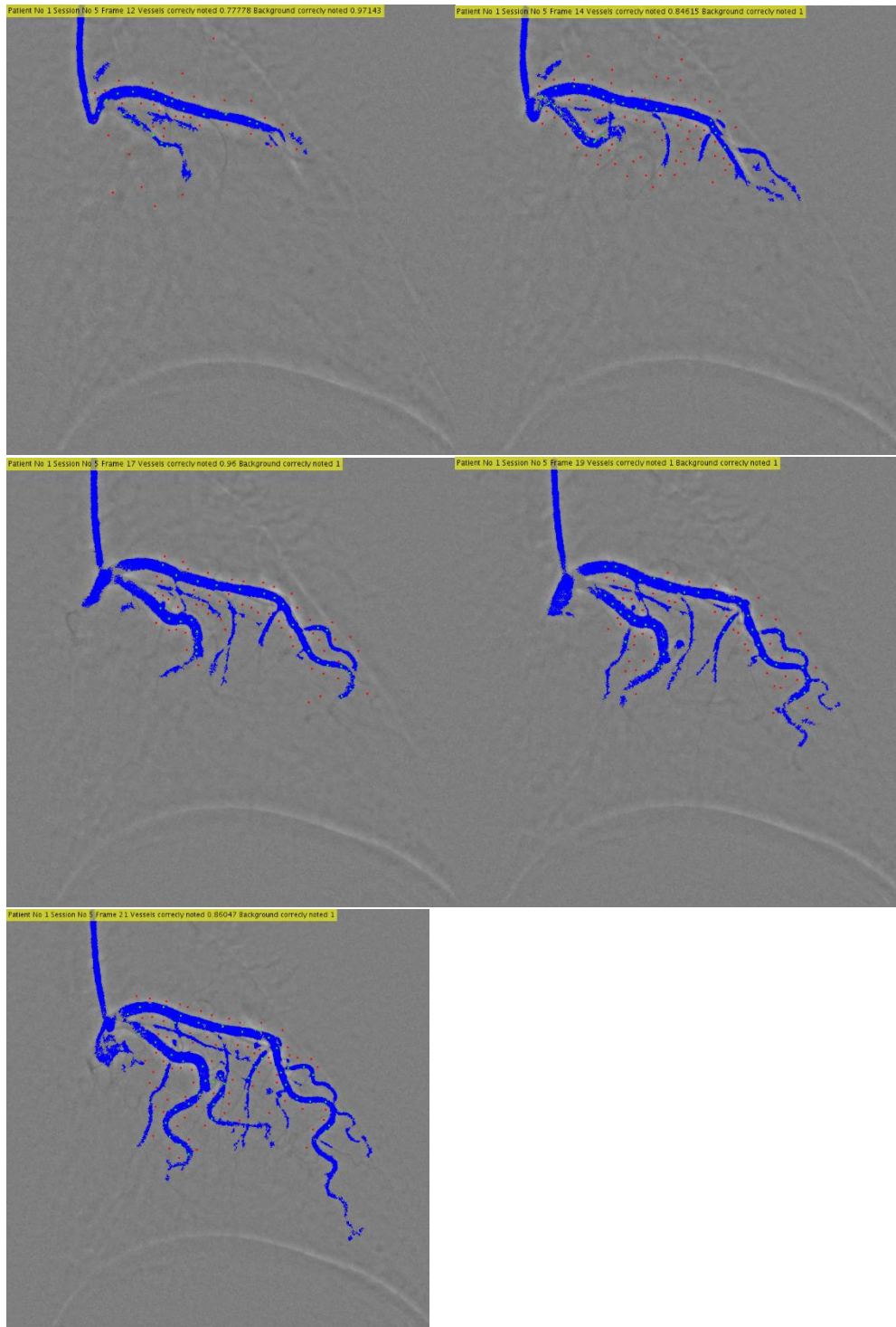
Truth table:

| Frame | Background segment detected | Vessel segment detected |
|-------|-----------------------------|-------------------------|
| 12 | 0.97 | 0.77 |
| 14 | 1.00 | 0.85 |
| 17 | 1.00 | 0.96 |
| 19 | 1.00 | 1.00 |
| 21 | 1.00 | 0.86 |

Flow Calculation and static dynamic mask



Final segmentations images



4.2 Patient 2: Session 4

Comment: Image had very clear contrast and allowed low noise trash to

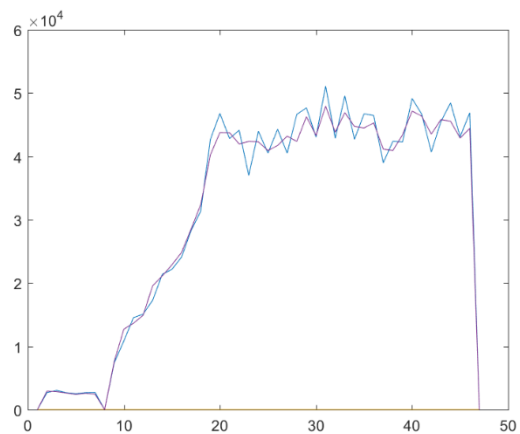
Parameters:

| | |
|------------------------------|------|
| Homomorphic Sigma | 25 |
| BinImgNoiseTresh1 | 0.01 |
| BinImgNoiseTresh2 | 0.02 |
| BinImgNoiseTresh3 | 0.05 |
| SuperpixelOccupancyThreshold | 0.25 |
| Number of smoothing | 0 |
| Dynmasktresh | 5.5 |

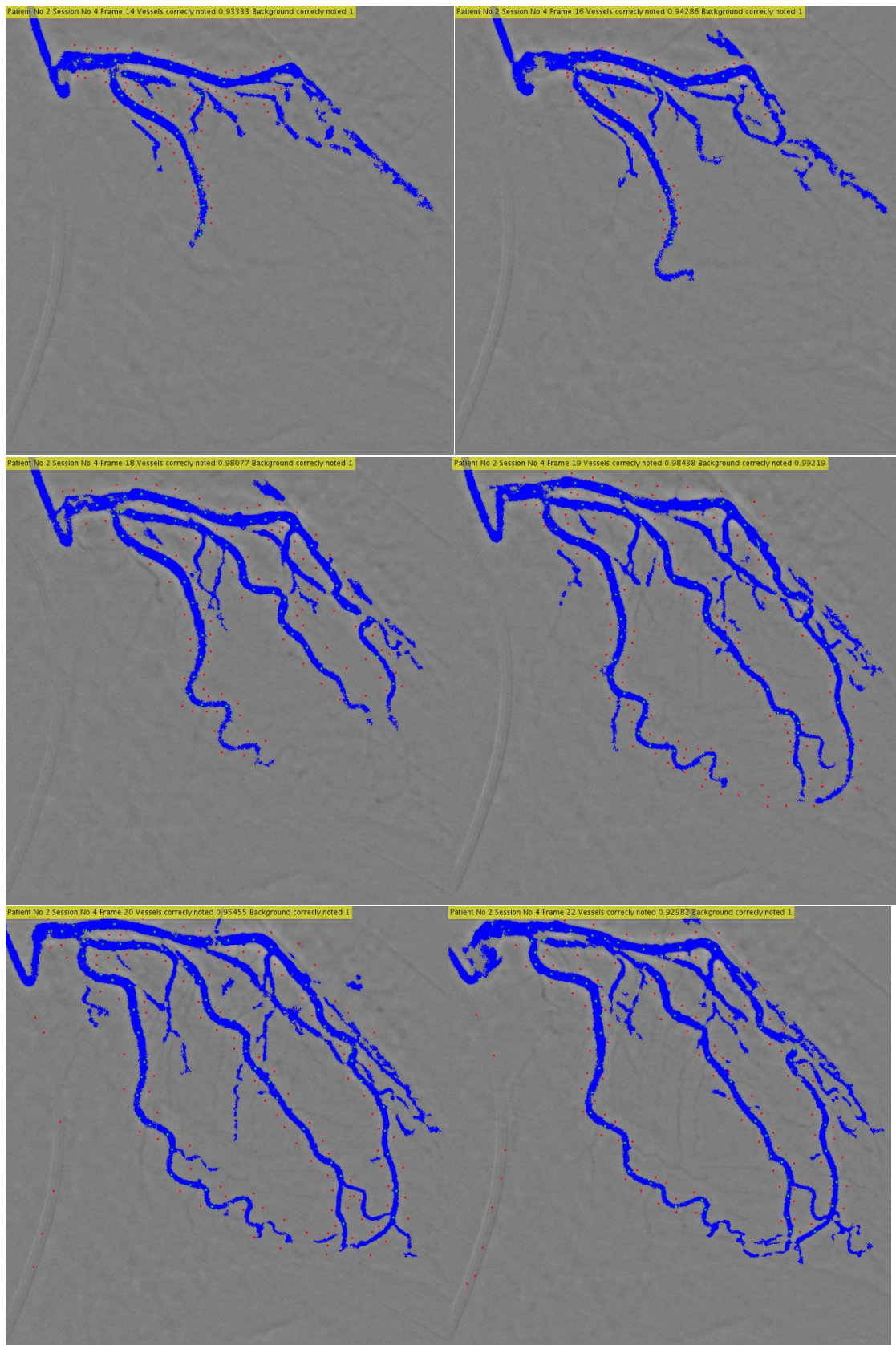
Truth table:

| Frame | Background segment detected | Vessel segment detected |
|-------|-----------------------------|-------------------------|
| 14 | 0.93 | 1.00 |
| 16 | 0.94 | 1.00 |
| 18 | 0.98 | 1.00 |
| 19 | 0.98 | 0.99 |
| 20 | 0.95 | 1.00 |
| 22 | 0.93 | 1.00 |

Flow Calculation and static dynamic mask



Final segmentations images



4.3 Patient 4: Session 2

Comment: Image had very clear contrast and allowed low noise trash to

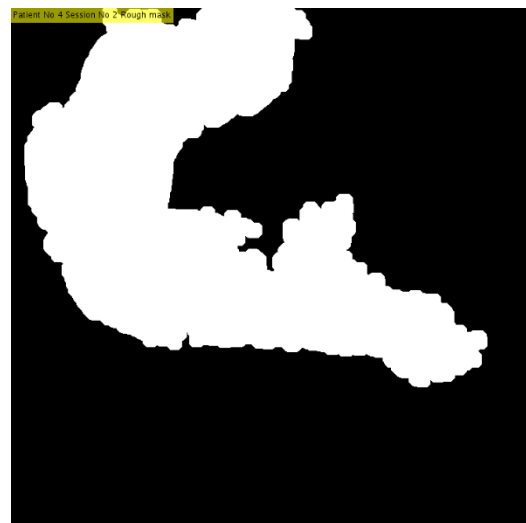
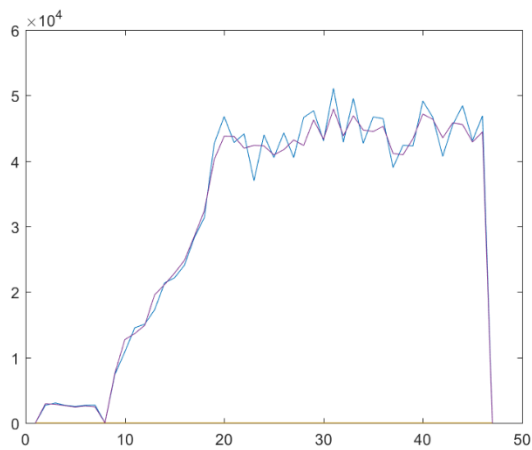
Parameters:

| | |
|-----------------------------|------|
| Homomorphic Sigma | 25 |
| BinImgNoiseTresh1 | 0.02 |
| BinImgNoiseTresh2 | 0.05 |
| BinImgNoiseTresh3 | 0.10 |
| SupapixelOccupancyThreshold | 0.40 |
| Number of smoothing | 1 |
| Dynmasktresh | 5.5 |

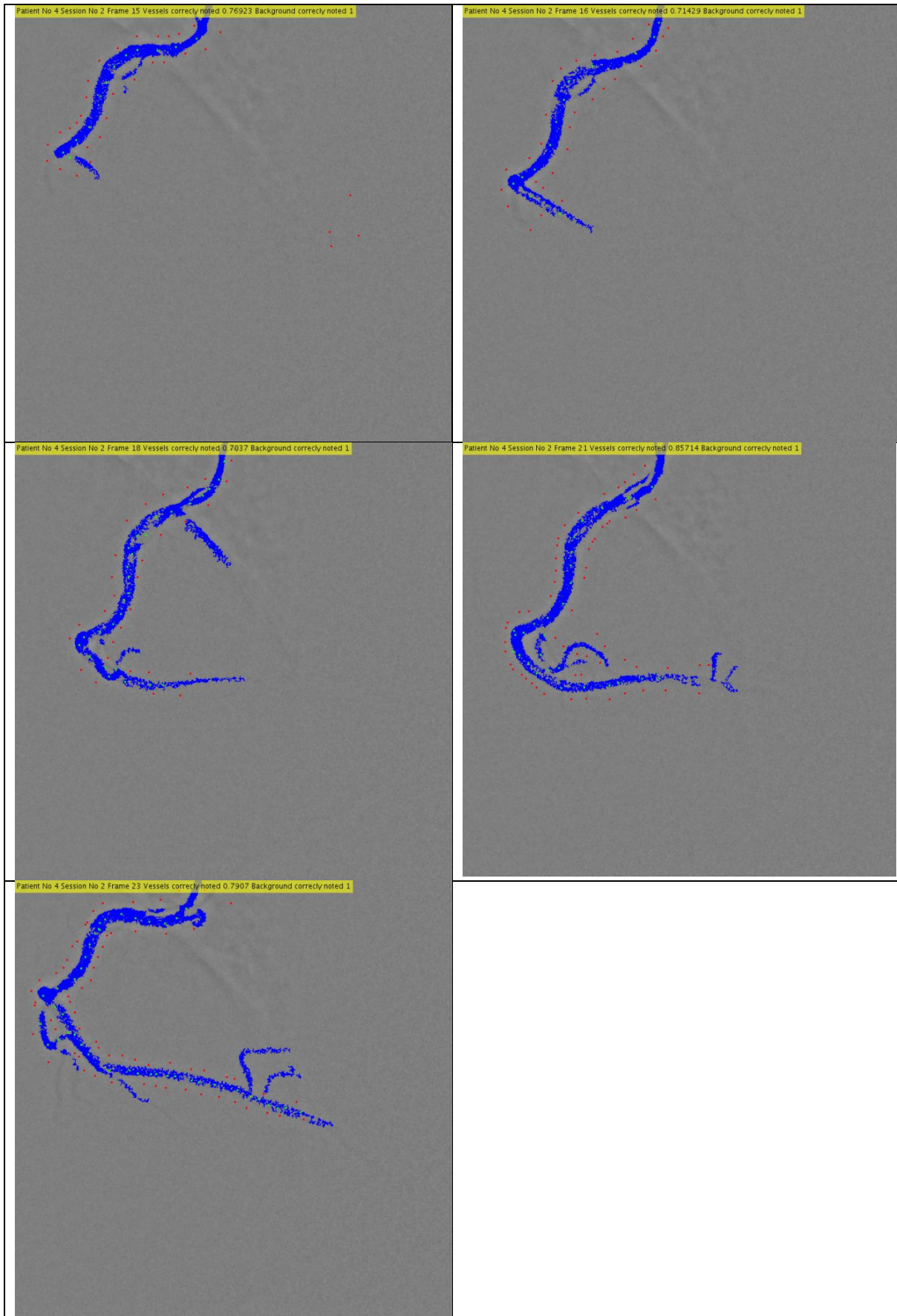
Truth table:

| Frame | Background segment detected | Vessel segment detected |
|-------|-----------------------------|-------------------------|
| 15 | 0.77 | 1.00 |
| 16 | 0.71 | 1.00 |
| 18 | 0.70 | 1.00 |
| 21 | 0.85 | 0.99 |
| 23 | 0.79 | 1.00 |

Flow Calculation and static dynamic mask



Final segmentations images



4.4 Patient 5: Session 2

Comment: Image had very clear contrast and allowed low noise trash to

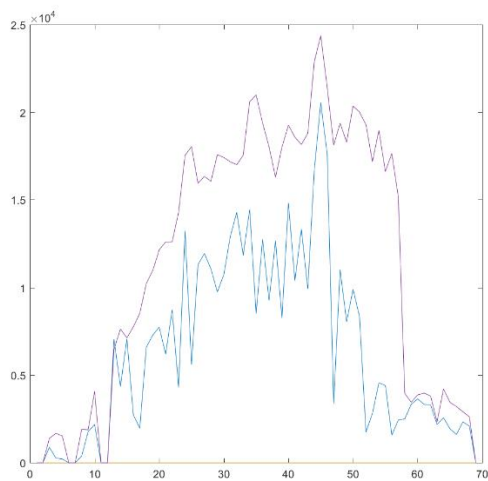
Parameters:

| | |
|-----------------------------|------|
| Homomorphic Sigma | 25 |
| BinImgNoiseTresh1 | 0.02 |
| BinImgNoiseTresh2 | 0.04 |
| BinImgNoiseTresh3 | 0.08 |
| SupapixelOccupancyThreshold | 0.25 |
| Number of smoothing | 1 |
| Dynmasktresh | 4.5 |

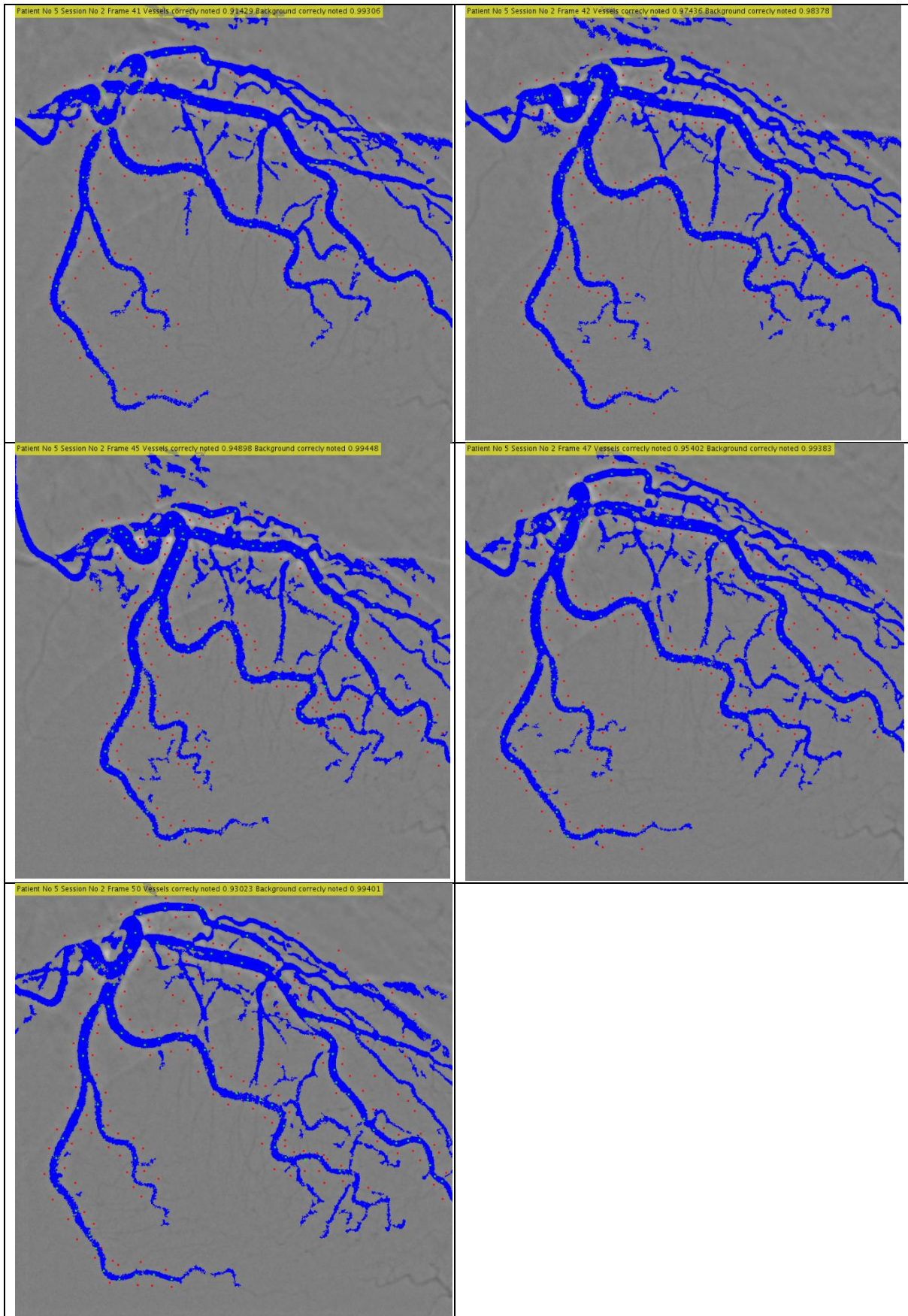
Truth table:

| Frame | Background segment detected | Vessel segment detected |
|-------|-----------------------------|-------------------------|
| 41 | 0.91 | 1.00 |
| 42 | 0.97 | 1.00 |
| 45 | 0.95 | 1.00 |
| 47 | 0.95 | 1.00 |
| 50 | 0.93 | 1.00 |

Flow Calculation and static dynamic mask



Final segmentations images



4.5 Patient 6: Session 5

Comment: Image had low contrast and large gap between insertion needle and contrast agent showing up on image

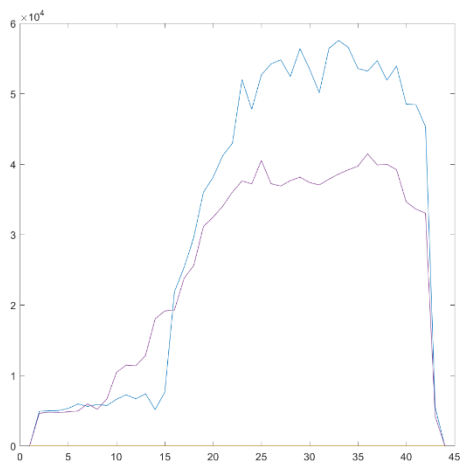
Parameters:

| | |
|------------------------------|----------------------|
| Homomorphic Sigma | 25 |
| BinImgNoiseTresh1 | 0.01 |
| BinImgNoiseTresh2 | 0.02 |
| BinImgNoiseTresh3 | 0.05 |
| SuperpixelOccupancyThreshold | 0.25 |
| Number of smoothing | 2 |
| Dynmasktresh | 4.5 + manual removal |

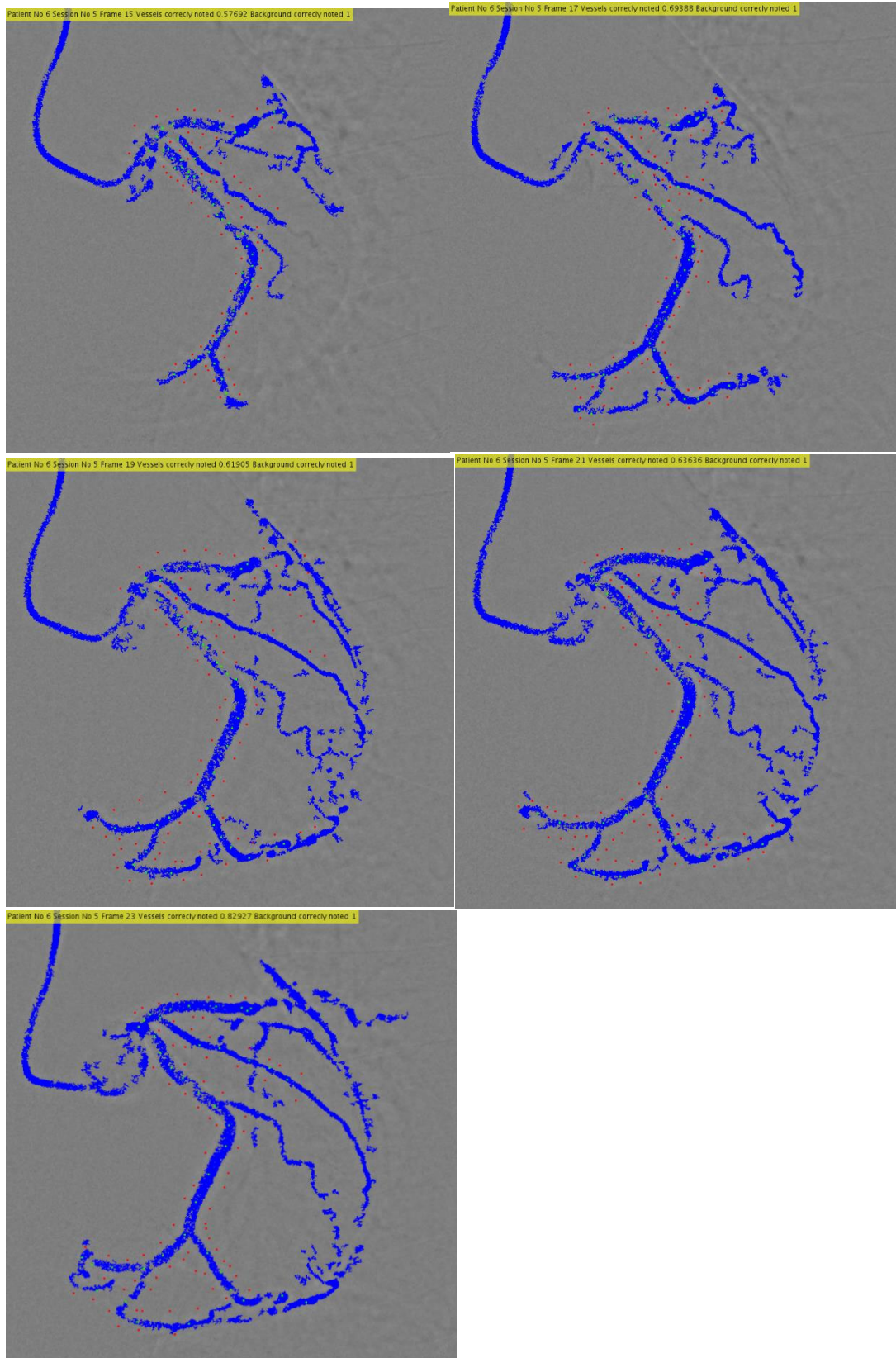
Truth table:

| Frame | Background segment detected | Vessel segment detected |
|-------|-----------------------------|-------------------------|
| 15 | 0.83 | 1.00 |
| 17 | 0.63 | 1.00 |
| 19 | 0.62 | 1.00 |
| 21 | 0.69 | 1.00 |
| 23 | 0.83 | 1.00 |

Binarization images:



Final segmentations images



4.6 Patient 7: Session 7

Comment: Image had very clear contrast and allowed low noise trash to

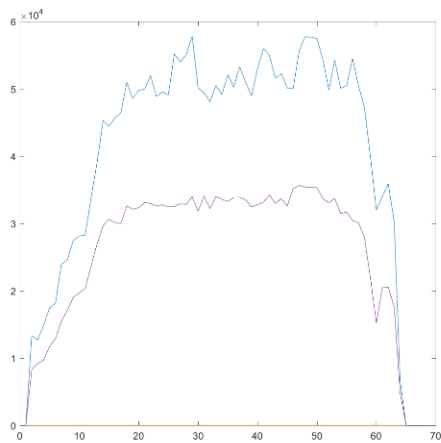
Parameters:

| | |
|------------------------------|-------|
| Homomorphic Sigma | 25 |
| BinImgNoiseTresh1 | 0.005 |
| BinImgNoiseTresh2 | 0.01 |
| BinImgNoiseTresh3 | 0.02 |
| SuperpixelOccupancyThreshold | 0.20 |
| Number of smoothing | 1 |
| Dynmasktresh | 6.5 |

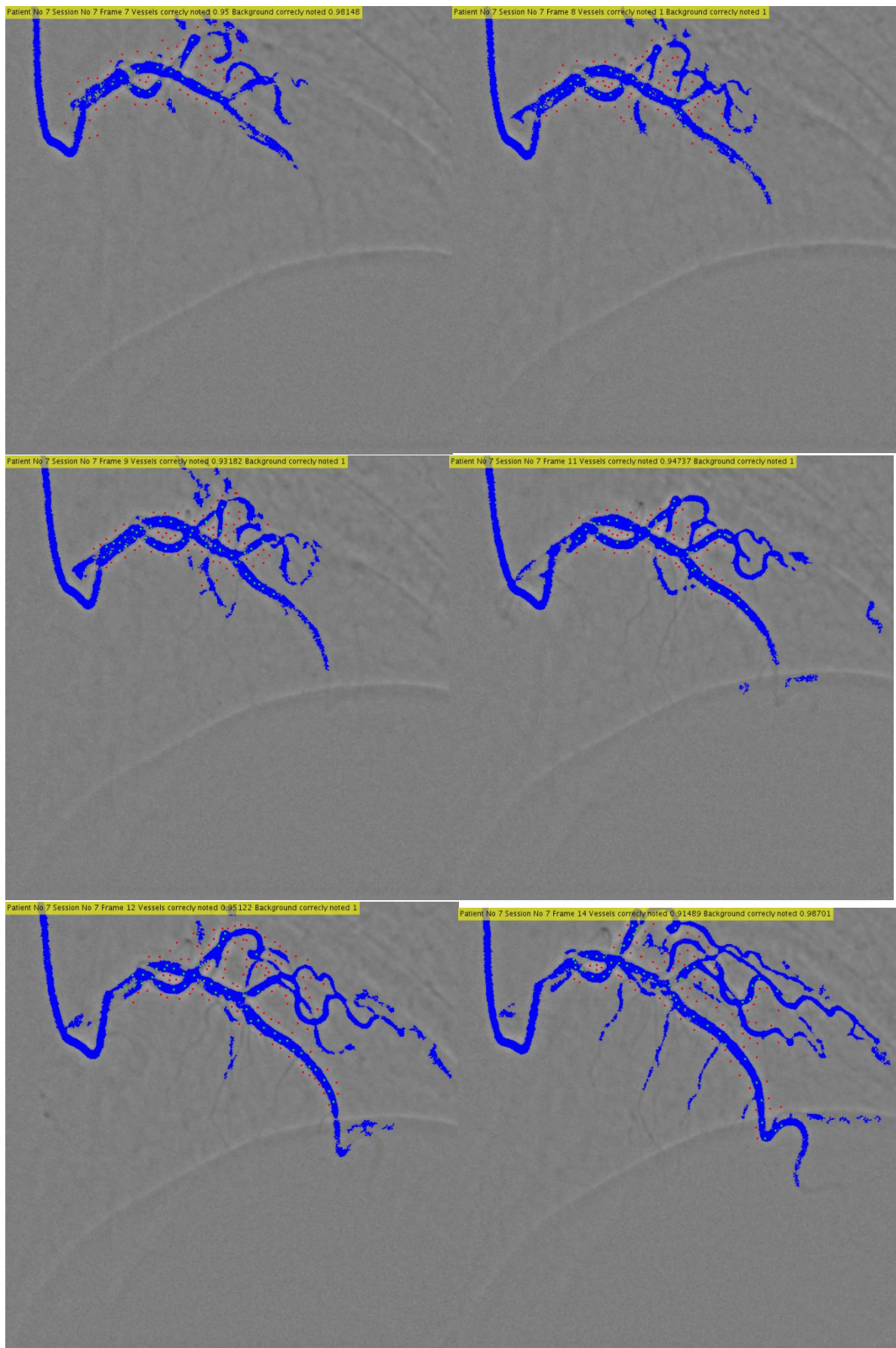
Truth table:

| Frame | Background segment detected | Vessel segment detected |
|-------|-----------------------------|-------------------------|
| 7 | 0.95 | 1.00 |
| 8 | 0.95 | 1.00 |
| 9 | 0.91 | 0.99 |
| 11 | 0.95 | 0.98 |
| 12 | 1.00 | 1.00 |
| 14 | 0.93 | 1.00 |

Flow Calculation and static dynamic mask



Final segmentations images



4.7 Patient 9: Session 4

Comment: Image had very clear contrast and allowed low noise trash to

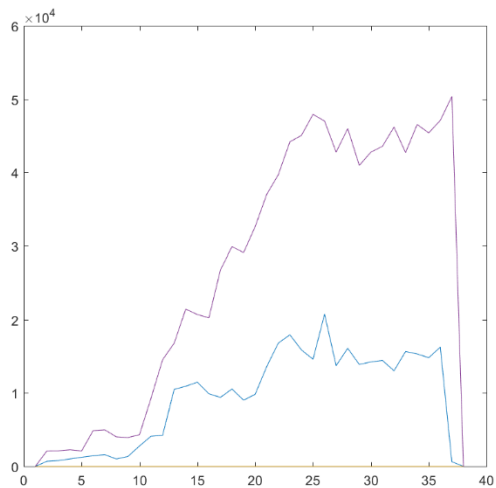
Parameters:

| | |
|------------------------------|------|
| Homomorphic Sigma | 25 |
| BinImgNoiseTresh1 | 0.01 |
| BinImgNoiseTresh2 | 0.02 |
| BinImgNoiseTresh3 | 0.04 |
| SuperpixelOccupancyThreshold | 0.7 |
| Number of smoothing | 1 |
| Dynmasktresh | 6.5 |

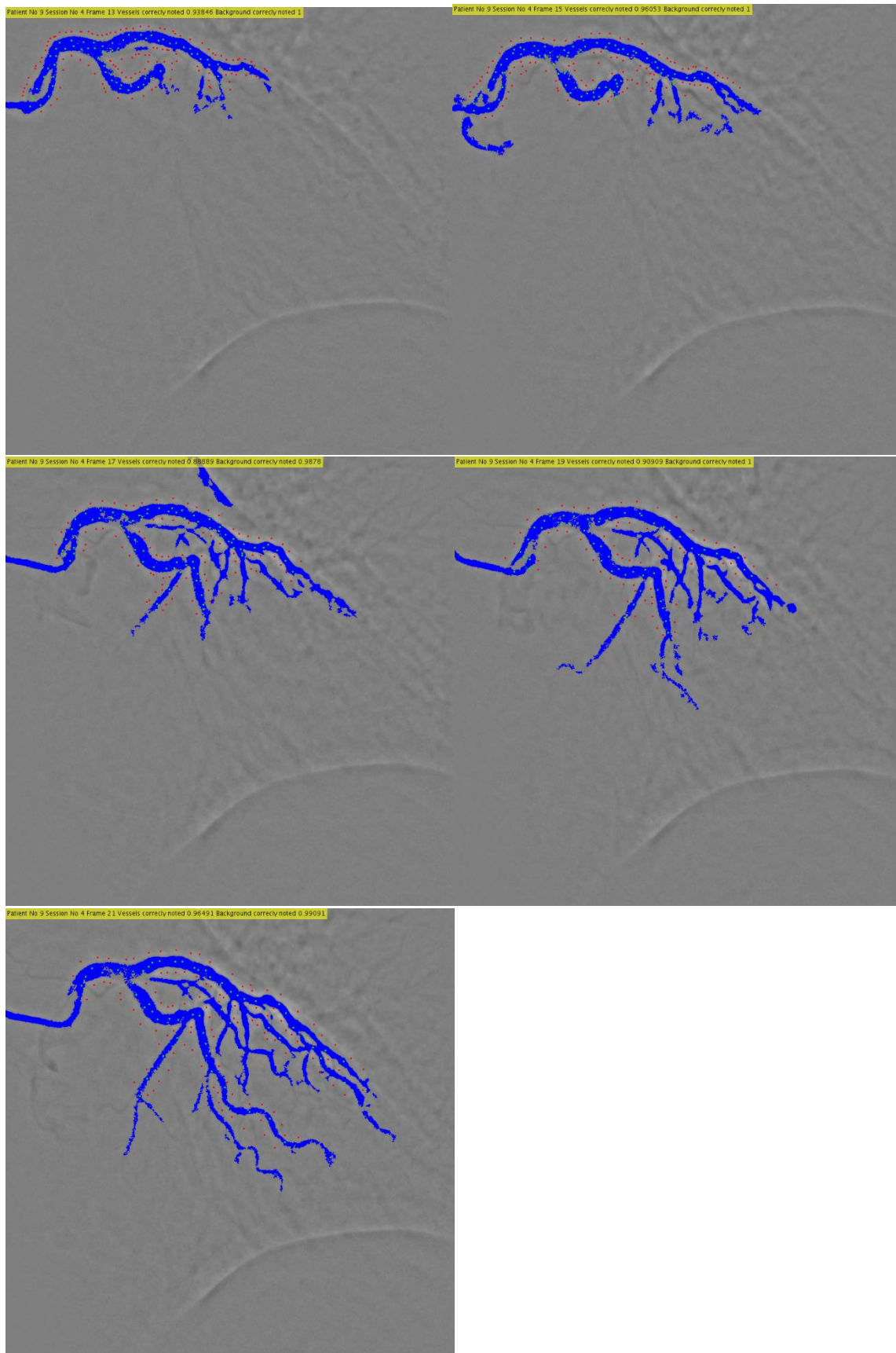
Truth table:

| Frame | Background segment detected | Vessel segment detected |
|-------|-----------------------------|-------------------------|
| 13 | 0.94 | 1.00 |
| 15 | 0.96 | 1.00 |
| 17 | 0.89 | 0.99 |
| 19 | 0.91 | 1.00 |
| 21 | 0.96 | 0.99 |

Flow Calculation and static dynamic mask



Final segmentations images



4.8 Patient 1: Session 5, Active contour adjustment

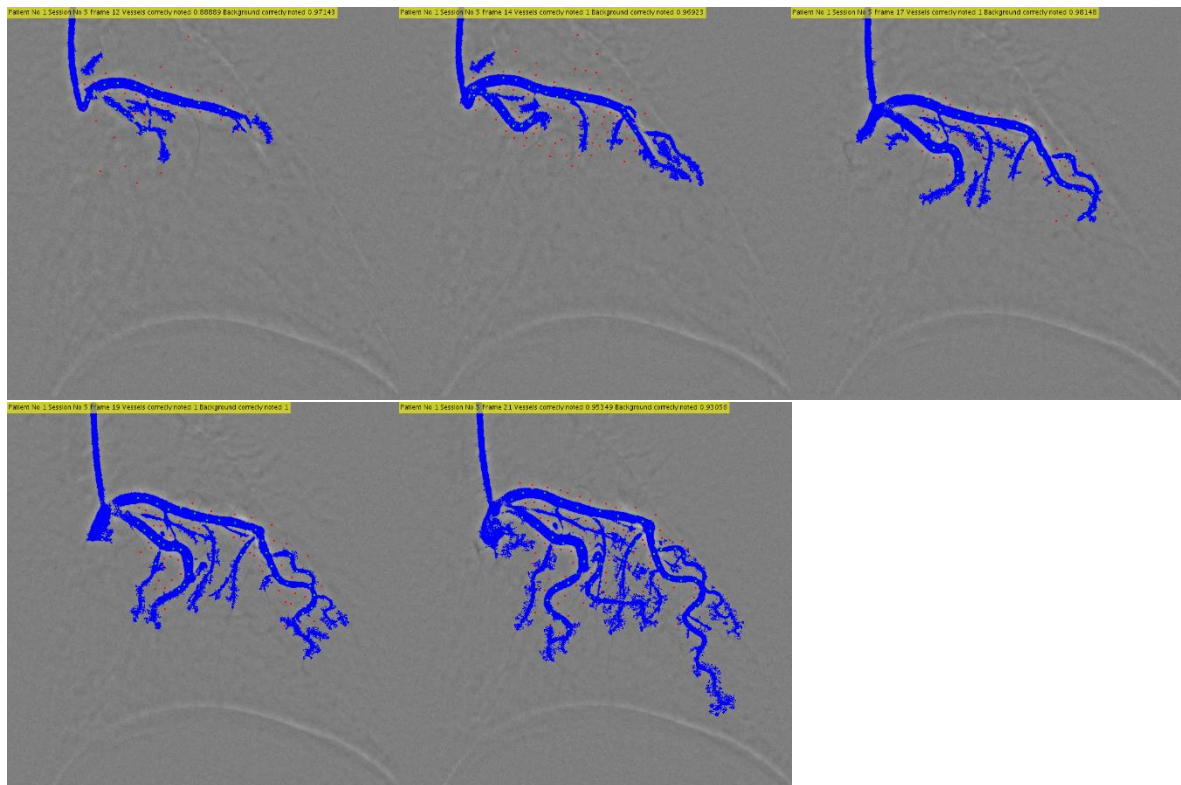
Comment: Final segmentation from 5.1 adjusted with active contour with homomorphic image and corrected with a binarization of mean image.

Parameters:

| | |
|------------------------------|------|
| Homomorphic Sigma | 25 |
| BinImgNoiseTresh1 | 0.01 |
| BinImgNoiseTresh2 | 0.02 |
| BinImgNoiseTresh3 | 0.05 |
| SuperpixelOccupancyThreshold | 0.25 |
| Number of smoothing | 0 |
| Dynmasktresh | 5.5 |
| Active conture bias | -0.3 |

Truth table:

| Frame | Background segment detected | Vessel segment detected |
|-------|-----------------------------|-------------------------|
| 12 | 0.97 | 0.88 |
| 14 | 0.97 | 1 |
| 17 | 0.98 | 1 |
| 19 | 1.00 | 1 |
| 21 | 0.93 | 0.9 |



4.9 Patient 1: Session 5, Watershed adjustment

Comment: Final segmentation used to extract watershed segments

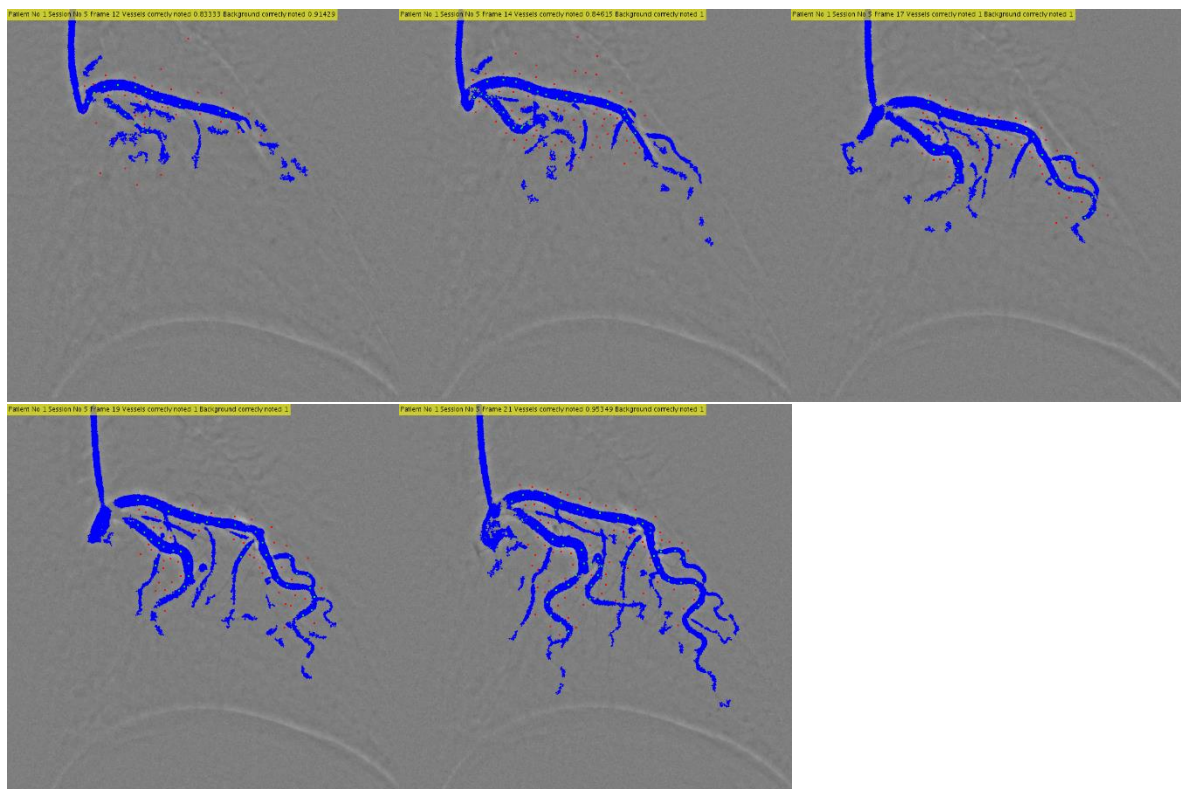
Parameters:

| | |
|------------------------------|-----------------------------|
| Homomorphic Sigma | 25 |
| BinImgNoiseTresh1 | 0.01 |
| BinImgNoiseTresh2 | 0.02 |
| BinImgNoiseTresh3 | 0.05 |
| SuperpixelOccupancyThreshold | 0.25 |
| Number of smoothing | 0 |
| Dynmasktresh | 5.5 |
| Water range | 0.01 to 0.21 0.2 increments |

Truth table:

| Frame | Background segment detected | Vessel segment detected |
|-------|-----------------------------|-------------------------|
| 12 | 0.91 | 0.83 |
| 14 | 1 | 0.85 |
| 17 | 1 | 1 |
| 19 | 1 | 1 |
| 21 | 1 | 0.95 |

Final segmentations images



5 Conclusion

The proposed method attempts to solve the problem very easily rather than following the methods from the norm that use advance models and looking for tubular shapes. Overall it succeeds well and a decent result can be achieved by simple preprocessing combined with smart segmentation and global thresholding. The results are only poor at low contrast images but consistently finds most of the main arteries. The proposed method is probably better to use as a supporting or initial function rather than a primary or sole method. I.e. watershed, active contours or Frangi hessian filtering to find a good threshold or to be used as initial segmentation method.

By expanding the methods to include information in the time domain and not only in the spatial domain as most papers concentrate on a lot of problems can be simplified given the camera is stationary during the video.

Finding a thresholding value over the time sequence by checking in the Static Dynamic Mask proved to generate a binarization of equal quality the entirety of the image sequence for this reason proved to generate more consistent images than histogram equalization or Otsu's method that resulted in varied result on a frame by frame basis and required varying degrees of blurring to make the binarization work.

There are some issues with the current implementation of the Static Dynamic Mask causing more seed points than needed and causing more points to be included in the super pixel growing.

The flaw of the proposed method as with most other studies is the problem to find the elusive thin vessels. The primary reason for this is the low resolution in the images that causes them to be presented with one or less pixel at the current low resolutions causing the need advance techniques that may not be needed with time. As the resolution of the images increase this will ease the proposed threshold method as well as the established firangi hessian method. As 2048x2048 with 100 fps x-ray video is available [18]. A rough comparison means that each pixel in a 736x736 image is substituted by almost 8 in 2048x2048. And in the case of 4k that would become almost 31 pixels.

6 References

- [1] SSB, Statistisk sentral byrå, "Statestikker, døde, år," 2016. [Online]. Available: <https://www.ssb.no/befolkning/statistikker/dode/aar/2016-03-09#content>.
- [2] Folke helse instetuttet, "Hjerte og karsykdommer i norge," [Online]. Available: <https://www.fhi.no/nettpub/hin/helse-og-sykdom/hjerte--og-karsykdommer-i-norge---f/>.
- [3] Folke helse instetuttet statestikkbank, "Døde år," [Online]. Available: <http://statistikkbank.fhi.no/dar/>.
- [4] M. Khanmohammadi, "Title: Extracting coronary arteries in angiography videos," 2016.
- [5] C. K. a. F. Quek, "A Review of Vessel Extraction Techniques," [Online]. Available: <http://www.siu.edu/~sumbaug/RetinalProjectPapers/Review%20of%20Blood%20Vessel%20Extraction%20Techniques%20and%20Algorithms.pdf>.
- [6] MATLAB, "correcting-nonuniform-illumination," [Online]. Available: <https://se.mathworks.com/help/images/examples/correcting-nonuniform-illumination.html>.
- [7] W. J. N. K. L. V. M. A. V. Alejandro F. Frangi, "Multiscale vessel enhancement filtering," [Online]. Available: <http://www.tecn.upf.es/~afrangi/articles/miccai1998.pdf>.
- [8] D.-J. Kroon, "hessian-based-frangi-vesselness-filter," [Online]. Available: <https://se.mathworks.com/matlabcentral/fileexchange/24409-hessian-based-frangi-vesselness-filter>.
- [9] T.-S. C. A. P.-C. C. PING-SUNG LIAO, "A Fast Algorithm for Multilevel Thresholding," [Online]. Available: http://www.iis.sinica.edu.tw/JISE/2001/200109_01.pdf.
- [10] P. T. T. M. A. K. Y.-K. L. S. L. T.-S. Kim, "Vessel enhancement filter using directional filter bank," [Online]. Available: http://uclab.khu.ac.kr/resources/publication/J_72.pdf.
- [11] R. M. K. Namuduri., "Gabor filter-based edge detection," [Online]. Available: <http://www.sciencedirect.com/science/article/pii/S030439900121121X>.
- [12] S. Eddins, "homomorphic-filtering-part 1," [Online]. Available: <https://blogs.mathworks.com/steve/2013/06/25/homomorphic-filtering-part-1/>.
- [13] S. Eddins, "homomorphic-filtering-part-2," [Online]. Available: <http://blogs.mathworks.com/steve/2013/07/10/homomorphic-filtering-part-2/>.
- [14] A. S. K. S. A. L. Radhakrishna Achanta, "SLIC Superpixels," [Online]. Available: http://www.kev-smith.com/papers/SLIC_Superpixels.pdf.
- [15] G. F. I. E. M. Caroline Lacoste, "CORONARY TREE EXTRACTION FROM X-RAY ANGIOGRAMS," [Online]. Available: <http://ieeexplore.ieee.org/document/1624876/>.

- [16] A. B. A. I. o. t. a. w. Leon, "Watershed-Based Segmentation and Region Merging," [Online]. Available: <http://www.sciencedirect.com/science/article/pii/S1077314299908226>.
- [17] L. A. V. T. F. Chan, "Active contours without edges. IEEE Transactions on Image Processing, Volume 10, Issue 2, pp. 266-277, 2001," [Online].
- [18] hamamatsu, "hamamatsu," 2017. [Online]. Available: https://www.hamamatsu.com/resources/pdf/sys/SCAS0011E_M11427.pdf.